

Point-by-point reply to the comments

Dear reviewer and top editor:

We would like to thank you for the time and effort spent in reviewing the manuscript. In response, we have carefully addressed your concerns with this work. Please see point-by-point response to the comments and the revised manuscript for details. The reviewer's and top editor's comments are shown in black *italics*. Our replies are shown in indented black text.

Sincerely

Yinchang Feng and co-authors

Content

Response to one anonymous Referee.....	1
RE1	1
Response to Topical editor Klaus Klingmüller	5
TE1	5
TE2	6
TE3	13
TE4	14
TE5	20
TE6	32
TE7	36
TE8	37
TE9	39
TE10.....	40
TE11.....	42
TE12.....	48
TE13.....	49
TE14.....	50
TE15.....	51
TE16.....	56
Reference	59

Response to one anonymous Referee

RE1

As one reviewer points out, there is still need for clarification regarding the chemical equilibrium of ions in the model: "In the PM_{2.5} source profiles (Sect 2.2), the chemical components (Ca, K, Mg, Mn, Na) are expressed in the form of element. In the aerosol thermodynamic process (Sect. 5), cations (Na⁺, Ca²⁺, K⁺, Mg²⁺) are used. Are all those elemental components (Ca, K, Mg, Mn, Na) from source emissions assumed to take part in the thermodynamic process in the form of cations (Na⁺, Ca²⁺, K⁺, Mg²⁺)? If so, are there any other anions used to make an ion balance with them? Are the cations and anions in equilibrium in the source profile as well as in the ISORROPIA simulation?"

We thank the reviewer for pointing this out. To address the reviewer's comment, we added further explanation as follows:

Source profile, the physical and chemical characterization of primary sources, characterizes specific sources from a physicochemical point of view which reveals the signatures of source emissions (Bi et al., 2019). Generally, the PM_{2.5} samples emitted from the sources are collected on Teflon and quartz fiber filters and then sent for chemical component analysis. Elements analysis uses Teflon filters, common chemical analysis instruments are: inductively coupled plasma optical emission spectrometer (ICP-OES), inductively coupled plasma atomic emission spectrometer (ICP-AES), inductively coupled plasma mass spectrometer (ICP-MS) instruments and X-ray fluorescence. The total carbon (TC) mass in the samples are typically determined using thermal or thermal–optical methods. There are two widely utilized approaches to dividing OC and EC from TC, known as IMPROVE_A (from the Desert Research Institute–DRI) and NIOSH (method 5040; from the National Institute for Occupational Safety and Health – NIOSH), which are operationally defined by the time–temperature protocols, and the OC–EC split point is determined by optical reflectance/transmittance

(Ho et al., 2003; Bi et al., 2019). PM samples collected on the quartz fiber filters are normally used for the determination of water-soluble inorganic ions via different types of ion chromatography (IC) with high-capacity cation-exchange and anion-exchange columns. Taking the two databases of source profiles mentioned in this paper as examples, in SPAP Database, the PM_{2.5} experiment analytical items contain 20 inorganic elements, 9 water-soluble ions, OC and EC (Details could be seen in Table TE1 as follows); And in SPECIATE database, it includes bulk species (SO₄²⁻, NO₃⁻, EC, OC, NH₄⁺, NCOM, MO, H₂O, PMO) and 37 trace elements (Na, Mg, Al, Si, P, S, Cl, K, Ca, Ti, V, Cr, Mn, Fe, Co, Ni, Cu, Zn, Ga, As, Se, Br, Rb, Sr, Zr, Mo, Pd, Ag, Cd, In, Sn, Sb, Ba, La, Ce, Hg, Pb) (Reff et al., 2009). **Source profile has been used extensively to determine the emission source by fingerprinting the traced chemical components not compounds. Ion equilibrium is not well considered in PM_{2.5} source profile**, as some ions which are not tested or not included due to technical limits.

Table TE1 Chemical components analysis of PM_{2.5} in SPAP

Items	Analysis method	Instrument
Na, Mg, Al, Si, K, Ca, Ti, V, Cr, Mn, Fe, Ni, Cu, Zn, Pb, As, Cd, Co, Hg, S	ICP	Thermo iCAP 7000
SO ₄ ²⁻ , NO ₃ ⁻ , F ⁻ , Cl ⁻ , K ⁺ , Ca ²⁺ , Na ⁺ , Mg ²⁺ , NH ₄ ⁺	ICS	Thermo ICS900
OC, EC	IMPROVE_A	DRI 2001A

Source: SPAP-Database of source profiles of air pollution, State Environmental Protection Key Laboratory of Urban Ambient Air Particulate Matter Pollution Prevention and Control & Tianjin Key Laboratory of Urban, Nankai University.

In CMAQ, the aerosol module (AERO6) expands the definition of the PM Other species in earlier versions to include more detailed PM species (Chapel Hill, 2012); There are 18 PM_{2.5} species in AERO6: OC, EC, SO₄²⁻, NO₃⁻, NH₄⁺, H₂O, Na, Cl, NCOM, Al, Ca, Fe, Si, Ti, Mg, K, Mn, and Other; Among them, for example, Na, K, Ca, Mg, NO₃⁻, Cl, and SO₄²⁻ participate in thermodynamic process (Calculate by ISORROPIA II, a thermodynamic equilibrium model); OC participate in gas phase chemistry and POA aging; Part of Fe and Mn take part in aqueous sulfur related

reactions; Si, Al, Ti and part of Fe represent crustal matter, undergo the microphysical processes and their deposition rates are determined within the aerosol module (Chapel Hill, 2012; Appel et al., 2013).

The generic solution procedure of ISORROPIA II (thermodynamic equilibrium model) is shown in the following Fig. TE1. **Inputs needed by ISORROPIA II are the total concentrations of Na, K, Ca, Mg, NH₃, HNO₃, HCl, and H₂SO₄** together with the ambient relative humidity and temperature (Nenes et al., 1998; Fountoukis and Nenes, 2007), **not all elemental components in source profile participate in thermodynamic process**. The elemental components (Ca, K, Mg, Mn, Na) from source emissions assumed to take part in the thermodynamic process, anions (like SO₄²⁻, NO₃⁻, Cl⁻, etc.) are used to balance with cations (Detail equilibrium relations are shown in Table TE2). The number of species and equilibrium reactions is determined by the relative abundance of each aerosol precursor (NH₃, Na, Ca, K, Mg, HNO₃, HCl, H₂SO₄) and the ambient relative humidity and temperature. The major species potentially present are determined by the value of R₁, R₂ and R₃. R₁, R₂ and R₃ are termed “total sulfate ratio”, “crustal species and sodium ratio” and “crustal species ratio” respectively; R₁'s value is determined by molar concentration of NH₄⁺, Ca²⁺, K⁺, Mg²⁺, Na⁺ and SO₄²⁻, R₂ is controlled by Ca²⁺, K⁺, Mg²⁺, Na⁺ and SO₄²⁻, R₃ is influenced by Ca²⁺, K⁺, Mg²⁺ and SO₄²⁻. Based on their values, aerosol composition regimes are defined. In ISORROPIA simulation, when the INPUT cations are changed, there must be some anions add in the system to balance with cations.

Our sensitivity experiment found that when the INPUT source profile (i.e. species allocation in emission sources) changed, for example, when we perturb an individual component in source profile, the influences are not only specific to this individual component, but also can be transmitted and linked among components, that is, the influence path is connected to chemical mechanisms in the model since the variation of species allocation in emission sources directly affect the thermodynamic equilibrium system (ISORROPIA II, SO₄²⁻-NO₃⁻-Cl⁻-NH₄⁺-Na⁺-K⁺-Mg²⁺-Ca²⁺-H₂O system).

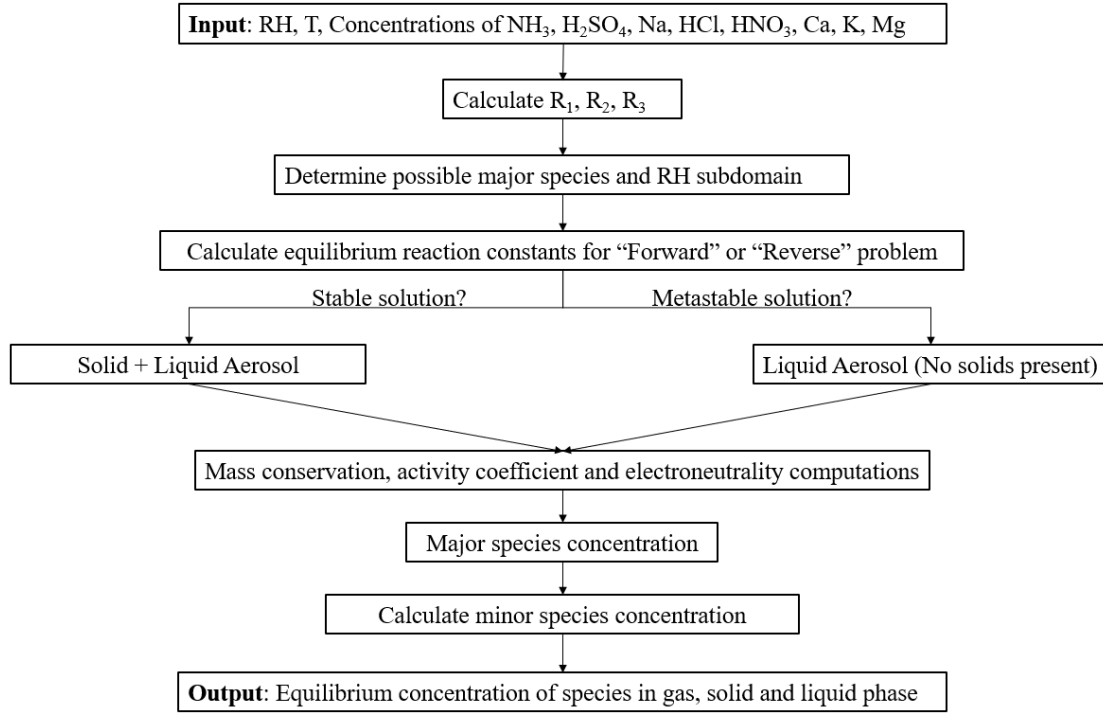


Fig. TE1 Generic solution procedure of ISORROPIA II

Table TE2 Equilibrium relations and K used in ISORROPIA II

Number	Reaction	K^0 (298.15K)
I1	$\text{Ca}(\text{NO}_3)_2(\text{s}) \leftrightarrow \text{Ca}_{(\text{aq})}^{2+} + 2\text{NO}_3(\text{aq})^-$	6.067×10^5
I2	$\text{Ca}(\text{Cl})_2(\text{s}) \leftrightarrow \text{Ca}_{(\text{aq})}^{2+} + 2\text{Cl}_{(\text{aq})}^-$	7.974×10^{11}
I3	$\text{CaSO}_4 \cdot 2\text{H}_2\text{O}(\text{s}) \leftrightarrow \text{Ca}_{(\text{aq})}^{2+} + \text{SO}_4(\text{aq})^{2-} + 2\text{H}_2\text{O}$	4.319×10^{-5}
I4	$\text{K}_2\text{SO}_4(\text{s}) \leftrightarrow 2\text{K}_{(\text{aq})}^+ + \text{SO}_4(\text{aq})^{2-}$	1.569×10^{-2}
I5	$\text{KHSO}_4(\text{s}) \leftrightarrow \text{K}_{(\text{aq})}^+ + \text{HSO}_4(\text{aq})^-$	24.016
I6	$\text{KNO}_3(\text{s}) \leftrightarrow \text{K}_{(\text{aq})}^+ + \text{NO}_3(\text{aq})^-$	0.872
I7	$\text{KCl}(\text{s}) \leftrightarrow \text{K}_{(\text{aq})}^+ + \text{Cl}_{(\text{aq})}^-$	8.680
I8	$\text{MgSO}_4(\text{s}) \leftrightarrow \text{Mg}_{(\text{aq})}^{2+} + \text{SO}_4(\text{aq})^{2-}$	1.079×10^5
I9	$\text{Mg}(\text{NO}_3)_2(\text{s}) \leftrightarrow \text{Mg}_{(\text{aq})}^{2+} + 2\text{NO}_3(\text{aq})^-$	2.507×10^{15}
I10	$\text{Mg}(\text{Cl})_2(\text{s}) \leftrightarrow \text{Mg}_{(\text{aq})}^{2+} + 2\text{Cl}_{(\text{aq})}^-$	9.557×10^{21}
I11	$\text{HSO}_4(\text{aq})^- \leftrightarrow \text{H}_{(\text{aq})}^+ + \text{SO}_4(\text{aq})^{2-}$	1.015×10^{-2}
I12	$\text{NH}_3(\text{g}) \leftrightarrow \text{NH}_3(\text{aq})$	57.64

I13	$\text{NH}_{3(\text{aq})} + \text{H}_2\text{O}_{(\text{aq})} \leftrightarrow \text{NH}_{4(\text{aq})}^+ + \text{OH}_{(\text{aq})}^-$	1.805×10^{-5}
I14	$\text{HNO}_{3(\text{g})} \leftrightarrow \text{H}_{(\text{aq})}^+ + \text{NO}_{3(\text{aq})}^-$	2.511×10^6
I15	$\text{HNO}_{3(\text{g})} \leftrightarrow \text{HNO}_{3(\text{aq})}$	2.1×10^5
I16	$\text{HCl}_{(\text{g})} \leftrightarrow \text{H}_{(\text{aq})}^+ + \text{Cl}_{(\text{aq})}^-$	1.971×10^6
I17	$\text{HCl}_{(\text{g})} \leftrightarrow \text{HCl}_{(\text{aq})}$	2.5×10^3
I18	$\text{H}_2\text{O}_{(\text{aq})} \leftrightarrow \text{H}_{(\text{aq})}^+ + \text{OH}_{(\text{aq})}^-$	1.010×10^{-14}
I19	$\text{Na}_2\text{SO}_{4(\text{s})} \leftrightarrow 2\text{Na}_{(\text{aq})}^+ + \text{SO}_{4(\text{aq})}^{2-}$	0.4799
I20	$(\text{NH}_4)_2\text{SO}_{4(\text{s})} \leftrightarrow 2\text{NH}_{4(\text{aq})}^+ + \text{SO}_{4(\text{aq})}^{2-}$	1.817
I21	$\text{NH}_4\text{Cl}_{(\text{s})} \leftrightarrow \text{NH}_{3(\text{g})} + \text{HCl}_{(\text{g})}$	1.086×10^{-16}
I22	$\text{NaNO}_{3(\text{s})} \leftrightarrow \text{Na}_{(\text{aq})}^+ + \text{NO}_{3(\text{aq})}^-$	11.97
I23	$\text{NaCl}_{(\text{s})} \leftrightarrow \text{Na}_{(\text{aq})}^+ + \text{Cl}_{(\text{aq})}^-$	37.66
I24	$\text{NaHSO}_{4(\text{s})} \leftrightarrow \text{Na}_{(\text{aq})}^+ + \text{HSO}_{4(\text{aq})}^-$	2.413×10^4
I25	$\text{NH}_4\text{NO}_{3(\text{s})} \leftrightarrow \text{NH}_{3(\text{g})} + \text{HNO}_{3(\text{g})}$	4.199×10^{-17}
I26	$\text{NH}_4\text{HSO}_{4(\text{s})} \leftrightarrow \text{NH}_{4(\text{aq})}^+ + \text{HSO}_{4(\text{aq})}^-$	1.383
I27	$(\text{NH}_4)_3\text{H}(\text{SO}_4)_2(\text{s}) \leftrightarrow 3\text{NH}_{4(\text{aq})}^+ + \text{HSO}_{4(\text{aq})}^- + \text{SO}_{4(\text{aq})}^{2-}$	29.72

Source: (Fountoukis and Nenes, 2007)

Response to Topical editor Klaus Klingmüller

TE1

Title: It seems inappropriate to speak of an "underappreciated" impact of the source profiles. While a realistic representation of emission sources may be challenging, the importance of source profile data is certainly appreciated. The meaning of "profile" in the context of this study should be clarified in the abstract and also in the title. A possible title might be "The effect of emission source chemical profiles on simulated PM_{2.5} components: sensitivity analysis with CMAQ 5.0.2".

Thank you for your advice. We have revised the title as “The effect of emission

source chemical profiles on simulated PM_{2.5} components: sensitivity analysis with CMAQ 5.0.2”

We also add the meaning of “profile” in the abstract. “Still, the emission source profiles (used to create speciated emission inventories for CTMs) of PM_{2.5} has not been fully taken into account in current numerical simulation.”

Detail shows as following screenshots 1-2:

Screenshot 1:

1 ~~The underappreciated impact of emission source profiles on the simulation of~~
2 ~~PM_{2.5} components: New evidence from sensitivity analysis~~ The effect of emission
3 source chemical profiles on simulated PM_{2.5} components: sensitivity analysis
4 with CMAQ 5.0.2⁴

Screenshot 2:

28 cause inaccurate simulation results. Still, the emission source profile (used to create
29 speciated emission inventories for CTMs) of PM_{2.5} has not been fully taken into account
30 in current numerical simulation. This study aims to answer (1) Whether the variation of
31 source profile adopted in CTMs has an impact on the simulation of PM_{2.5} chemical
32 components? (2) How much does it impact? (3) How does the impact work? Based on

TE2

Line 22: The claim that "current models do not perform very well in simulating PM_{2.5} components" is too general and does not reflect the literature.

Thank you for your suggestion. we have revised the original sentence as “current models do not perform very well in reproducing the observations of some major chemical components, for example, sulfate, nitrate, ammonium and organic carbon”. To address your comment, we add an extra explanation as follows:

Based on our summary of published relevant literatures, the normalized mean bias (NMB) of sulfate, nitrate, ammonium and organic carbon are highly variable and inconsistent between the simulated and the observed values to some extent (SO₄²⁻:

84%~98%; NO_3^- : -80%~118%; NH_4^+ : -58%~130%; OC: -73%~43%; As Fig. TE2 shows below). We have also collected some published literatures to further elaborate this conclusion, and the references are listed in Table TE3 (Table S1 in supplementary material). Detailed information has been supplemented in the introduction of the revised manuscript.

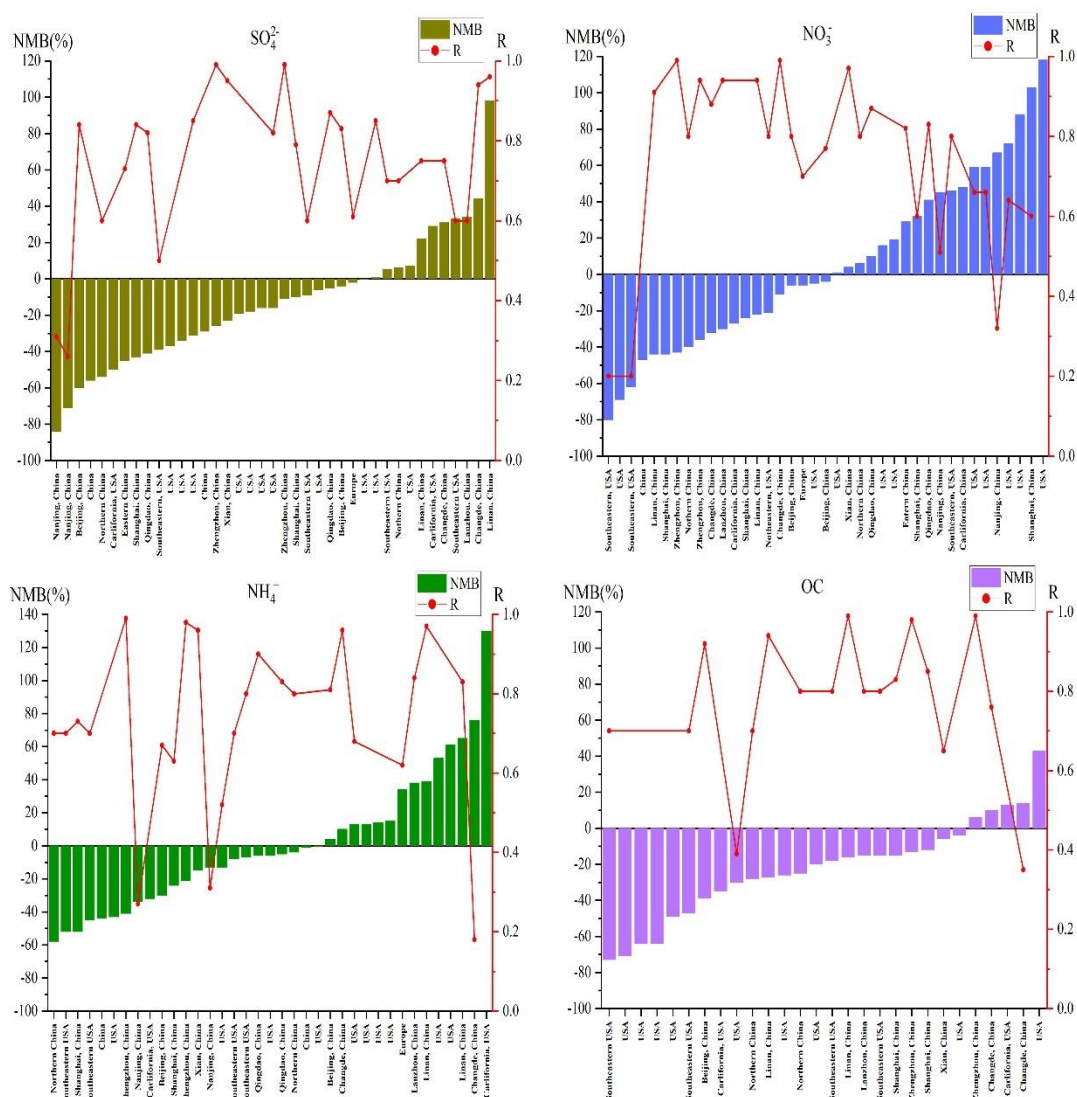


Fig. TE2 The normalized mean bias (NMB) between the simulated and the observed values in some literatures

Table TE3 The simulation error of CTMs on the components of PM_{2.5} in different studies

PM _{2.5} components	Model	NMB	R	Study area	Period	Reference
SO ₄ ²⁻	CMAQv4.7.1	-45%	0.73	Eastern China	2010	(Cheng et al., 2015)
NO ₃ ⁻		29%	0.82			
SO ₄ ²⁻	CMAQv4.7.1	-4.5%	0.87	Qing Dao	Jan. 2016	(Zhang et al., 2017)
NO ₃ ⁻		10%	0.87			
NH ₄ ⁺		-6%	0.9			
SO ₄ ²⁻	CMAQv5.0.1	-54%	0.6	Northern China	2013	(Zheng et al., 2015)
NO ₃ ⁻		-40%	0.8			
NH ₄ ⁺		-58%	0.7			
OC		-25%	0.8			
EC		196%	0.6			
SO ₄ ²⁻	Revised CMAQ	6%	0.7	Northern China	2013	(Zheng et al., 2015)
NO ₃ ⁻		6%	0.8			
NH ₄ ⁺		-4%	0.8			
OC		-28%	0.7			
EC		183%	0.6			
SO ₄ ²⁻	WRF-Chem3.6.1	-84%	0.31	Nanjing	Jan. 2017	(Sha et al., 2019)
		-71%	0.26		Apr. 2017	
NO ₃ ⁻		45%	0.51		Jan. 2017	
		67%	0.32		Apr. 2017	

NH ₄ ⁺		-34%	0.27		Jan. 2017	
		-13%	0.31		Apr. 2017	
SO ₄ ²⁻	CMAQv5.0.2	-41%	0.82	Qing Dao	Dec. 2015 ~ Jan. 2016	(Gao et al., 2020)
NO ₃ ⁻		41%	0.83			
NH ₄ ⁺		-5%	0.83			
SO ₄ ²⁻	RAQMS	-4%	0.83	Beijing	Feb. to Mar. 2014	(Li et al., 2020)
NO ₃ ⁻		-4%	0.77			
NH ₄ ⁺		4%	0.81			
OC		-39%	0.92			
EC		-9%	0.81			
SO ₄ ²⁻	CMAQv5.0.1	-56%~-29%	-	China	2013	(Shi et al., 2017)
NO ₃ ⁻		-47%~19%				
NH ₄ ⁺		-44%~1				
SO ₄ ²⁻	CMAQv4.7	-16% and -6%	-	USA	Jan. 2006	(Foley et al., 2010)
SO ₄ ²⁻		-19%~-0.2%			Aug. 2006	
		NO ₃ ⁻			-5% and 1%	
NH ₄ ⁺		13% and 14%			Jan. 2006	
		15% and -6%			Aug. 2006	
OC		-20%			Jan. 2006	
		-49%			Aug. 2006	
EC		-25%			Jan. 2006	
	-32%	Aug. 2006				

SO ₄ ²⁻	CMAQv4.5.1	-34%~7%	-	USA	Jan. 2002	(Liu et al., 2010)
		-18%~-37%			Jul. 2002	
NO ₃ ⁻		16%~118%			Jan. 2002	
		-69%~88%			Jul. 2002	
NH ₄ ⁺		-0.5%~61%			Jan. 2002	
		-43%~53%			Jul. 2002	
OC		-4%~13%			Jan. 2002	
		-71%~-64%			Jul. 2002	
EC	-16%~18%	Jan. 2002				
	-39%~38%	Jul. 2002				
SO ₄ ²⁻	CMAQv4.5.1	5%	0.7	South Eastern USA	Jan. 2002	(Zhang et al., 2013)
	CAMx-4.4.2	33%	0.6		Jul. 2002	
	CMAQv4.5.1	-39%	0.5			
	CAMx-4.4.2	-9%	0.6			
NO ₃ ⁻	CMAQv4.5.1	46%	0.8		Jan. 2002	
	CAMx-4.4.2	-21%	0.8		Jul. 2002	
	CMAQv4.5.1	-62%	0.2			
	CAMx-4.4.2	-80%	0.2			
NH ₄ ⁺	CMAQv4.5.1	-7%	0.8	Jan. 2002		
	CAMx-4.4.2	-8%	0.7	Jul. 2002		
	CMAQv4.5.1	-52%	0.7			
	CAMx-4.4.2	-45%	0.7			

OC	CMAQv4.5.1	-15%	0.8		Jan. 2002			
	CAMx-4.4.2	-18%	0.8					
	CMAQv4.5.1	-73%	0.7		Jul. 2002			
	CAMx-4.4.2	-47%	0.7					
EC	CMAQv4.5.1	-9%	0.7		Jan. 2002			
	CAMx-4.4.2	5%	0.7					
	CMAQv4.5.1	-47%	0.4		Jul. 2002			
	CAMx-4.4.2	-33%	0.4					
SO ₄ ²⁻	CMAQv5.0	0.7% and -31%	0.85	USA	1990-2010	(Xing et al., 2015)		
		-2%	0.61	Europe				
NO ₃ ⁻		56%~59%	0.66	USA				
		-6%	0.70	Europe				
NH ₄ ⁺		-13%	0.52	USA				
		34%	0.62	Europe				
SO ₄ ²⁻		-16%	0.82	USA			2002~2008	(Friberg et al., 2016)
NO ₃ ⁻		72%	0.64					
NH ₄ ⁺	13%	0.68						
OC	-30%	0.39						
EC	-22%	0.5						
SO ₄ ²⁻	CMAQv5.0.2	-50%~29%	-	California	2013	(Chen et al., 2020)		
NO ₃ ⁻		-27%~48%						
NH ₄ ⁺		-32%~130%						

OC		-35%~13%				
EC		0~43%				

TE3

Line 33: You highlight that the effect of changes in the source profile on the simulated PM_{2.5} components cannot be ignored as a major result. However, the composition of the emissions obviously affects the composition of the pollution (it is the exact relationship which is less obvious due to chemistry). In addition, the percentages given in the abstract are of limited relevance as they only apply to a single site.

Thank you for your questions.

The chemical composition of ambient PM_{2.5} is influenced by both source emissions and atmospheric chemical reactions during transport. Source profile, species allocation in emission sources, is used to create speciated emission inventories for CTMs. In the reported literatures, PM_{2.5} species allocation coefficients of emission sources for CTMs are commonly treated by referring to source profile data in published literature or database like the US SPECIATE. However, with the development of production technology and the innovation of pollution treatment technology in recent years, the chemical composition of PM_{2.5} source emissions has changed. It is worth exploring whether the variation of source profile adopted in CTMs has a significant impact on the simulation results.

To our knowledge, this is the first study to date in response to the above issues. In our study, we separately selected source profiles from SPAPPC and SPECIATE databases and used them to create speciated emission inventories for CTMs. By designing a series of sensitivity experiments based on variations in source profile, we found the influence of source profile variation on the simulation of chemical components in PM_{2.5} could not be ignored. The simulation results of some components are sensitive to the adopted source profile in CTMs. In addition, there is a linkage effect, the variation of some components in source profile would bring changes to the simulated results of other components, since the variation of species allocation in emission sources directly affect the thermodynamic equilibrium system in CTMs.

In this study, we used CMAQ (one of the most widely used CTMs), MEIC (a high-

resolution inventory of anthropogenic air pollutants in China), meteorological field, simulation domain and monitoring sites as carriers to explore the influence of source profile changes on the simulation results. The same kind of experiment is also applicable to other CTMs, other emission source profiles, and other simulation domain.

We have rewritten this part in the abstract to make it more clearly expressed (The modified text is shown in corresponding screenshot 3 below).

Screenshot 3:

30 in current numerical simulation. This study aims to answer (1) Whether the variation of
31 source profile adopted in CTMs has an impact on the simulation of PM_{2.5} chemical
32 components? (2) How much does it impact? (3) How does the impact work? Based on
33 the characteristics and variation rules of chemical components in typical PM_{2.5} sources,
34 different simulation scenarios were designed and the sensitivity of simulated PM_{2.5}
35 componentselements-simulation results to PM_{2.5} sources chemical profile was
36 explored. Our findings showed that the influence of source profile changes on simulated
37 PM_{2.5} concentration was insignificant, but its impact on simulated PM_{2.5} components
38 could not be ignored. The variations of simulated components ranged from 8% to 167%
39 under selected different source profiles, and simulation. Simulation results of some
40 components were sensitive to the adopted PM_{2.5} source profile in CTMs. Moreover,
41 there was a linkage effect, the variation of some components in the source profile would
42 bring changes to the simulated results of other components. These influences are
43 connected to ~~the~~ chemical mechanisms of the model since the variation of species
44 allocations in emission sources ~~directly affected the~~ can affect potential composition
45 and phase state of aerosols, chemical reaction priority and multicomponent chemical
46 balance in thermodynamic equilibrium system. We also found that the perturbation of

TE4

The article still lacks information on how the MEIC emissions are combined with the source profiles.

Thank you for your comments. More descriptions have been added in Table S26 of our supplementary material. Please see the detail explanation as follows:

In the database of Source Profiles of Air Pollution (SPAP) and U.S. Environmental Protection Agency's (EPA) SPECIATE database, these four source categories (coal-

fired power plant, industry process, transportation sector and residential coal combustion) contain a series of sub-categories. But the MEIC emission inventory does not include the corresponding sub-categories. So we take the average values of source profiles in each source category as representing source profile (Table TE4), the details could also be seen in our previous work (Bi et al., 2019); Then multiply inventory emissions by profile fraction to get emissions of specific chemical components. The general step for speciation is shown in Fig. TE3.



Fig. TE3 Speciation in general step

Source: International Emissions Inventory Conference. SPECIATE and using the Speciation Tool to prepare VOC and PM chemical speciation profiles for air quality modeling, p31. https://www.epa.gov/sites/default/files/2017-10/documents/speciate_speciationtool_training.pdf.

The modified text is shown in corresponding screenshots 4 below:

Screenshot 4:

185 other sources, collected from more than 40 cities in China since 2001. In addition to
186 inorganic elements, water-soluble ions, OC, EC and other conventional components,
187 some source profiles also encompass a series of tracer information, such as organic
188 markers, isotopes, single particle mass spectrometry, VOCs and other gaseous
189 precursors. Based on species in the aerosol chemical mechanism (AERO6) of CMAQ
190 (Appel et al., 2013; Chapel Hill, 2012), we selected 15 components in PM_{2.5} source
191 profiles including Al, Ca, Cl, EC, Fe, K, Mg, Mn, Na, OC, Si, Ti, NH₄⁺, NO₃⁻ and SO₄²⁻,
192 the remaining components are classified as “other”. ~~Emission sources are divided into~~
193 ~~four main categories referred to the classification in MEIC: coal combustion by power~~
194 ~~plants (PP), industrial processes (IN), residential emission (RE) and transportation~~
195 ~~sector (TR). In the database of Source Profiles of Air Pollution (SPAP) and U.S.~~
196 ~~Environmental Protection Agency’s (EPA) SPECIATE database, these four source~~
197 ~~categories (coal-fired power plant, industry process, transportation sector and~~
198 ~~residential coal combustion) contain a series of sub-categories. But the MEIC emission~~
199 ~~inventory does not include the corresponding sub-categories. So we take the average~~
200 ~~values of source profiles in each source category as representing source profile, the~~
201 ~~details could also be seen in our previous work (Bi et al., 2019); Then multiply~~
202 ~~inventory emissions by profile fraction to get emissions of specific chemical~~
203 ~~components.~~ ↵

Table TE4 The selected information of source profile in SPECIATE and SPAPPC database

Code	Profile Name	Controls	Profile Date	Profile Notes	Keywords	Match MEIC source ^e
91041 ^a	Draft Sub-Bituminous Combustion - Composite	Mixture of Baghouse, None, Electrostatic Precipitator, Wet Scrubber, Mechanical Collectors, Dry Lime Scrubber, Ammonia Injection	2006-5-24	Replaced by Profile 91110. Median of Profiles 3191, 3192, 3690, 3694, and 3700.	Sub-Bituminous Coal Combustion; PM Composite	PP
900162.5 ^b	Industrial Manufacturing - Average	Not Applicable	1989-1-5	Average profile developed from original profiles representing the source category group 3xxxxxxx.	INDUSTRIAL	IN
91155 ^c	Residential Coal Combustion - Composite	Uncontrolled	2009-7-12	Median of Profiles 3761, 432012.5	Residential Coal Combustion; Inventory speciation	RE
91022 ^a	Draft On-road Gasoline Exhaust - Composite	Mixture of Catalytic converter and Not available	2006-5-24	Replaced by Profile 91122. Median of Profiles 311072.5, 3517, 3884, 3892,	On-road Gasoline Exhaust; PM Composite	TR

91162 ^c	LDDV Exhaust - Composite	Mixture of Catalytic converter and Not available	2009-7-12	3904, 3947, 3951, 3955, 3959, and 4558. Median of Profiles 321042.5, 3912, 3963, 4675	LDDV Exhaust; Inventory speciation
Local ^d	Coal combustion by power plants	Mixture of Baghouse, None, Electrostatic Precipitator, Wet Scrubber, Mechanical Collectors, Dry Lime Scrubber,		Average of profiles power and heating power plant	PP
Local ^d	Industrial processes	Wet Scrubber, Dry Lime Scrubber,		Average of profiles steel, metallurgy, cement, glass, industrial boiler	IN
Local ^d	Transportation sector	Mixture of Catalytic converter		Average of profiles gasoline, diesel, gasoline-diesel exhaust	TR
Local ^d	Residential emission			Average of profiles civil boiler	RE

a, Hsu, Ying, Randy Strait, Stephen Roe, David Holoman. 2006. 'SPECIATE 4.0 Speciation database development document - Final Report', Prepared for US EPA, RTP, NC, EPA Contract Nos. EP-D-06-001, Work Assignment Numbers 0-03 and 68-D-02-063, WA 4-04 and WA 5-05, by E.H. Pechan & Associates, Incorporation, Durham, NC. https://www.epa.gov/sites/production/files/2015-10/documents/speciatedoc_1206.pdf.

b, Shareef, G. S. Engineering Judgement, Radian Corporation. August 1987.

c, Reff, Adam, Prakash V Bhave, Heather Simon, Thompson G Pace, George A Pouliot, J David Mobley, and Marc Houyoux. 2009. 'Emissions Inventory of PM_{2.5} Trace Elements across the United States', Environmental Science & Technology, 43, no. 15: 5790-96. DOI: 10.1021/es802930x.

d, Database of Source Profiles of Air Pollution (SPAP), measured by State Environmental Protection Key Laboratory of Urban Ambient Air Particulate Matter Pollution Prevention and Control & Tianjin Key Laboratory of Urban, Nankai University.

e, Coal combustion by power plants (PP), industrial processes (IN), residential emission (RE) and transportation sector (TR).

TE5

Figs. 2 to 5: Please clarify that the figures present statistics of profiles from different data sources. It would be helpful to include all profiles considered - including the SPAP profiles - in Tables S3 to S11. Figs. 2 to 5 could be combined into one figure with four panels.

Thank you for your advice. We have clarified the figures present statistics of profiles from different data source and added the SPAP profiles data in our supplementary material (Table S3 to S11), Table TE5~TE13 below. Figs. 2 to 5 are combined into one figure (Fig. TE4) in the revised manuscript. Details could also be seen as follows:

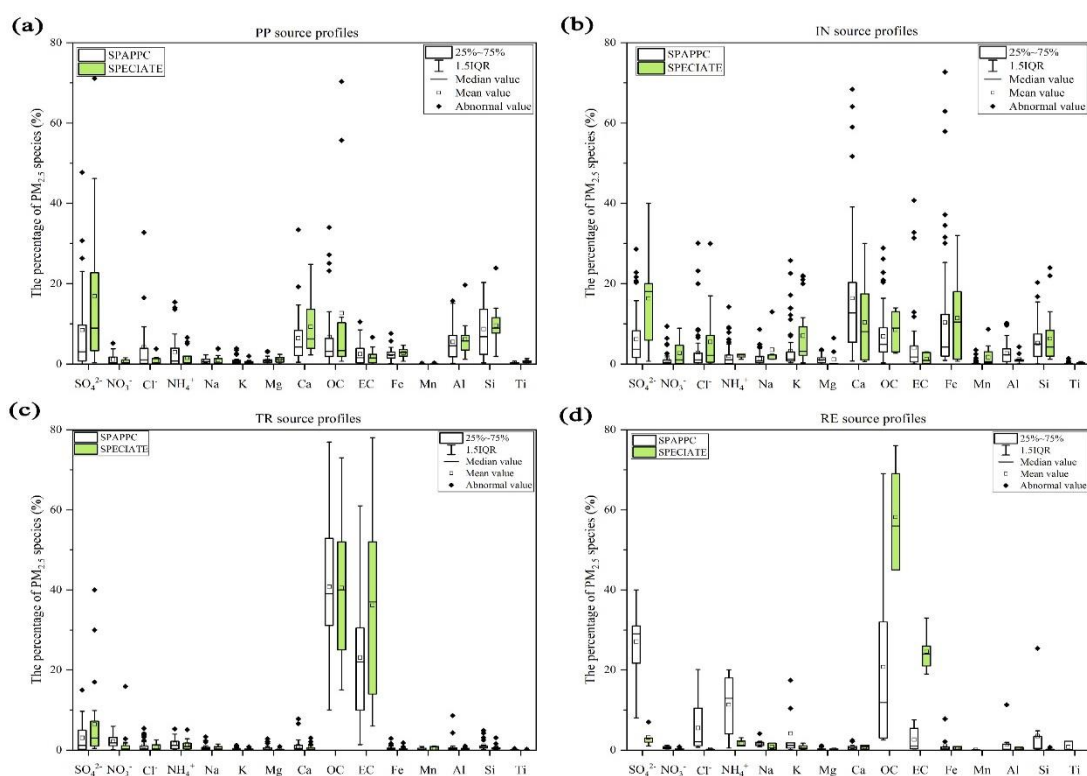


Fig. TE4 Chemical profiles for PM_{2.5} emitted from (a) coal-fired power plant (PP), (b) industry processes (IN), (c) transportation sector (TR), (d) residential coal combustion (RE). Data obtained from SPAPPC (SPAP database and published source profiles in China) and SPECIATE (U.S. EPA SPECIATE database)

Table TE5 Power plant source profiles from published literatures in China, SPAP and SPECIATE database

Year	SO ₄ ²⁻	NO ₃ ⁻	Cl ⁻	NH ₄ ⁺	Na	K	Mg	Ca	OC	EC	Fe	Mn	Al	Si	Ti	Other	City/Region	Data source
2005~2006	2.9	0.6	3.4	0.1	1	0.3	0.5	2.5	34	4	2	0.05	1.7		0.1	46.9	Southern China	(Liu, 2007)
2006	23		0.7	4			0.7	5.5	2	0.3	2		4.2			57.6	Shang Hai	.(Zheng et al., 2013)
2009~2013	0.8	0.2	0.1		0.3	0.8		1.7	0.3	1.8	2		15.1	20.3	0.6	56	Shijiazhuang	(Qi et al., 2015)
2012	5.8	1.5	1.8	0.6	1	2.6	2	3	13	0.4	0.9	0.03	2.3	12.8	0.1	52.2	Beijing	(Ma et al., 2015)
2013	2.4	0.2		0.03	2.2	0.2	0.9	8.8	4	0.8	0.8	0.04	5.7	7.5		66.4	Changzhou	(Teng et al., 2015)
2015~2016	8.7	0.9	16.5	4.9	2.1	3.9	1.1	9.6	4.2	0.4	2.3	0.1	1.3	2.4	0.1	41.7	Tianjin	(Bi et al., 2019)
2017	7.8		9.3		0.2	0.1	0.2	3.6	1.4	0.1	1.6		2.2	15.2		58.3	Yantai	(Wen et al., 2019)
	3.2		9.2	3.0	0.5	0.2	1.1	19.3	6.7	0.7	2.6	0.1	3.0	3.0	0.1	47		SPAP, Bi et al. 2019
	10.1	0.1	32.8	14.0	0.2	0.1	0.8	0.9	1.9	0.3	0.2	0.01	0.2	2.1	0.01	36		SPAP, Bi et al. 2019
	0.03	0.3	0.1	0.5	0.03	0.1	0.04	1.1	0.1	0.05	0.2	0.003	0.8	0.6	0.03	96		SPAP, Bi et al. 2019
	9.4	2.1	3.9	1.5	0.9	0.7	3.2	33.4	0.1	0.1	2.7	0.1	4.2	0.8	0.04	37		SPAP, Bi et al. 2019
	30.7	3.8	1.1	15.4	0.8	0.4	1.6	3.4	27.2	4.3	3.0	0.1	9.7	3.8	0.3			SPAP, Bi et al. 2019
	26.4	3.7	1.0	13.6	1.4	0.6	3.1	6.4	23.2	3.5	3.6	0.1	15.7	12.1	0.4			SPAP, Bi et al. 2019
	0.5	0.1	0.04	2.4		0.3	0.3	1.7	1.1	1.4	2.9	0.04	4.8	4.8	0.3	79		SPAP, Bi et al. 2019
	0.3	0.02	0.1	0.05		0.6	0.5	3.2	1.9	4.0	3.5	0.03	8.0	11.3	0.5	66		SPAP, Bi et al. 2019
	0.8	0.1	0.4	0.03		0.5	0.4	4.8	2.1	3.8	3.8	0.1	6.9	6.2	0.4	70		SPAP, Bi et al. 2019
	1.7	0.1	1.5	0.1	0.1	0.9	0.8	6.8	1.9	3.4	5.8	0.2	13.8	11.9	0.7	50		SPAP, Bi et al. 2019
	0.9	0.04	0.3	0.03	0.2	1.1	1.0	8.0	2.6	3.3	7.6	0.2	14.9	10.1	0.7	49		SPAP, Bi et al. 2019
			0.03	0.2	0.4	0.6	0.5	5.3	7.9	5.1	2.2	0.03	7.1	20.3	0.3	50		SPAP, Bi et al. 2019
	2.7	0.3	0.4	0.7	0.6	0.6	0.6	5.0	6.1	10.5	2.9	0.03	5.1	14.2	0.3	50		SPAP, Bi et al. 2019
			0.03	0.1	0.7	0.6	0.9	12.3	5.5	8.5	2.6	0.04	6.5	13.6	0.3	48		SPAP, Bi et al. 2019
	1.8	0.3	0.2	0.2	0.3	0.4	0.4	3.4	2.0	5.8	2.6	0.04	7.3	20.0	0.4	55		SPAP, Bi et al. 2019
	0.1		0.0	0.2	0.4	0.4	0.4	3.6	2.6	3.6	2.2	0.03	6.3	20.0	0.3	60		SPAP, Bi et al. 2019

1987	10.2		0.1	0.3		0.5		3.5		4.3	2.9	0.03	6	9.0	0.4	62.9	Colorado	3190
1987	2.1		0.1	0.3		0.5		2.6	4.4	6.7	2.7	0.03	6.4	9.1	0.4	64.7	Colorado	3191
1987	18.2	0.1	0.1	0.4		0.4		4.3	1.9	1.9	3.1	0.02	5.5	8.9	0.5	54.6	Colorado	3192
1987	2.4		0.1	0.3		0.8		7.2	2.9	1.2	4.7	0.06	9	12.0	0.5	58.9	Colorado	3194
1995	27.3	0.2	0.2	2.0	2.1	0.8	2.4	3.8	3.2	2.2	3.3	0.12	4.2	7.8	0.2	40.1	Colorado	3687
1995	15.4	0.4	1.7	0.2	0.3	0.1	0.3	10.0	1.9	2.5	0.7	0.01	1.3	2.3	0.01	62.9	Colorado	3691
1995	7.7	0.2	1.6	6.6	0.1	0.4	0.5	2.3	11.7	1.7	1.9	0.01	5.4	9.0	0.4	50.5	Colorado	3700
1997	1.5		0.3		0.6	2.0	1.9	4.0	8.7	0.4	1.9	0.03	19.7	23.9		35.2	South Africa	3987
1999	10.2	1.6	3.8	0.3	3.8	0.6	1.2	4.3	70.3	0.01	0.8	0.03	1.2	1.9	0.1	0.03	Texas	4290
1999	71.1		0.2	5.5	0.1	0.3		5.4	1.0	0.2	2.3	0.08	2.8	8.5	0.5	2.2	Texas	4307
1999	41.5	0.1		0.8	0.2	0.6		24.8	3.6	0.9	4.4	0.3	2.1	12.5	1.4	6.7	Texas	4310
1999	4.3	1.3		0.1	0.2	0.1	1.7	21.8	0.7		3.7	0.1	7.4	7.6	1.0	50.0	Texas	4315
2002	5.7	1.0	0.3	0.5	0.4	0.2	1.3	16.1	55.7	2.4	2.9	0.03	5.6	6.1	0.6	1.2	Texas	4368
2002	46.2	0.1	1.1	5.1	0.1	0.5	0.1	11.1	10.3	0.1	3.7	0.2	6.5	13.9	0.8	0.2	Texas	4371
2002	6.4	0.7	0.0	0.1	0.2	0.3	1.5	18.8	1.5	1.4	3.5	0.1	6.8	9.1	1.0	48.6	Texas	4317
2006	12.7	0.2	0.07	0.4	0.1	0.4	0.5	3.7	2.6	1.9	2.7	0.02	5.4	8.9	0.4	60.0		91041
2010	0.4				3.9	0.3	0.0	8.5			2.0		9.5	11.2	0.6	63.7	Canada	95518

Note:

1. The values under different components are the weight percentage in $PM_{2.5}$, %; the number under data source represents the code number in `speciate_5.0_0`;
2. SPAP data used in this table were deposited to the Mendeley data repository and can be freely downloaded from <https://doi.org/10.17632/x8dfshjt9j.2>, Bi et al., 2019.

Table TE6 Industrial process (sintering) source profiles from published literatures in China, SPAP and SPECIATE database

Year	SO ₄ ²⁻	NO ₃ ⁻	Cl ⁻	NH ₄ ⁺	Na	K	Mg	Ca	OC	EC	Fe	Mn	Al	Si	Ti	Other	City/Region	Data source
2006	23		20.0	1.7	2.2	17.2	0.2	13	13		1.2	0.0				9.0	Shanghai	(Zheng et al., 2013)
2007	22	0.1	8.4	0.6	3.1	22.6	1.1	7	11	2.6	4.8	0.1	3.8	6.8	0.3	5.6		(Ma, 2009)
2007	6	0.1	7.1	0.1	4.3	3.2	3	15	9	3.3	30.1	0.7	5.9	9.2	0.4	2.4		
2012~2013	3	0.0	3.1	0.2	1.6	25.8	0.2	2	13	5.2	6.2	0.1	0.6	6.8		32.6		(Zhao, 2014)
2012~2013	7	0.2	6.6	0.1	0.4	7	0.5	5	10	3.4	25.3	0.2	2.9	9.2		22.7		
2012~2014					1.9	1.2	1.3	4	2		37.2	0.1	7.1	20.3	0.8	24.7	Guiyang	(Wang et al., 2016)
2015	13	0.5	23.2	8.9	2	13.9	0.1	17	6	0.3	2.7		0.1	0.1		12.7	Jing-Jin-Ji	(Guo et al., 2017)
2017	2	9	4	2	1	1	3	33	4	0.3	3	0.1	4	1	0.04	34		SPAP
2017	0.03	6	7	6	1	5	0.2	1			1	0.02	0.01	1	0.01	71		SPAP
2017	1	0.4	9	2	0.3	3	0.5	14	0.3	3	7	0.04	0.2	2	0.004	58		SPAP
2018	2	0.1	1	0.3	0.0004	1	0.4	13			35	1	1	5		41		SPAP
1988			0.3			0.3		13			27.5	0.7	2.6	6.4	0.3	49.2		283042.5
1989	20		17.0			20.0		1			13.0	0.6				28.8		283012.5
2009	10		17.0		13.0	21.0	0.2	1	3	0.2	6.9	0.3	0.1	1.2		26.8		91139

Note:

1. The values under different components are the weight percentage in PM_{2.5}, %; the number under data source represents the code number in speciate_5.0_0
2. SPAP: Database of Source Profiles of Air Pollution (SPAP, <http://www.nkspap.com:9091/>), measured by State Environmental Protection Key Laboratory of Urban Ambient Air Particulate Matter Pollution Prevention and Control & Tianjin Key Laboratory of Urban, Nankai University.

Table TE7 Industrial process (iron-making) source profiles from published literatures in China, SPAP and SPECIATE database

Year	SO ₄ ²⁻	NO ₃ ⁻	Cl ⁻	NH ₄ ⁺	Na	K	Mg	Ca	OC	EC	Fe	Mn	Al	Si	Ti	Other	City/Region	Data source
2007	12	2.6	6.6	1.1	4	4.4	2.9	6.5	12	0.8	14	0.4	10	17	0.7	5.5		(Ma, 2009)
2012~2013	29	1.3	1.5		2.8	12.2	0.8	4	5	1.3	32	0.3	1.2	2		7.6		(Zhao, 2014)
2014~2015	11	4.8		5.5	1.3	1.7	3.6	7.7	16	7	9	0.1	3.5	4	1.4	23.6		(Liu et al., 2017)
2015	7	0.5	1.6	2.3	0.9	3.2	0.2	2.5	4	4.2	63	0.8	0.3	1	0.2	8.3	Jing-Jin-Ji	(Guo et al., 2017)
2018	2		0.4	1.7				8.7	6	0.8	25			7		49.5	Wuhan	(Wen et al., 2018)
	6.1	1.6	5.2	2.7	1.7	3.3	1.3	7.7	8.2	7.8	12.8	0.3	2.0	2.7	0.2	37		SPAP
2017	2	0.02	0.2	1	0.2	1	0.1	6	6	3	17	0.1	1	1	0.02	62		SPAP
1989			2.5		2.0	3.2		2			6	1.70	1.3	2	0.5	79.5		282012.5
1989			0.9		1.3	3.0		1.0			15	4.50	1.1	24	0.1	49.1		282022.5
1989			1.7		1.7	3.1		1.3			10	3.1	1.2	13	0.3	64.2		900102.5
2006	2	0.2			1.3	1.9	3.1	6.2	3	0.4	32	3.60	0.7	3	0.2	42.0		91011
2009	6	0.5	0.8		1.2	2.7		0.9	6	0.9	14	4.10	1.0	22	0.1	39.1		91157

Note:

1. The values under different components are the weight percentage in PM_{2.5}, %; the number under data source represents the code number in speciate_5.0_0
2. SPAP: Database of Source Profiles of Air Pollution (SPAP, <http://www.nkspap.com:9091/>), measured by State Environmental Protection Key Laboratory of Urban Ambient Air Particulate Matter Pollution Prevention and Control & Tianjin Key Laboratory of Urban, Nankai University.

Table TE8 Industrial process (steelmaking) source profiles from published literatures in China, SPAP and SPECIATE database

Year	SO ₄ ²⁻	NO ₃ ⁻	Cl ⁻	NH ₄ ⁺	Na	K	Mg	Ca	OC	EC	Fe	Mn	Al	Si	Ti	Other	City/Region	Data source
2010	0.9		1.1		1	1.3	3.5	8.7	4.2	1.6	16.6	0.1	5.3	8.9	0.3	46.5	Jincheng	(Cui, 2011)
2012~2013	14.1	0.5	2.2	0	2.8	11.1	1.6	2.2	2.3	1.5	6.4	3.5	0.6	2.5		48.7		(Zhao, 2014)
2012~2013	5.6	0.2	3.6	0	0.4	3.6	0.3	0.9	4.1	0.1	57.9	0.9	0.4	2.9		19.1		
2015	0.8		2.3		1.1	3	0.6	7.0	0.3		72.7	2.5	0.3	1.2	0.2	8	Jing-Jin-Ji	(Guo et al., 2017)
2018	1.4		0.3	2.0				20.3	8.8	0.7	8.2			11.0		47.3	Wuhan	(Wen et al., 2018)
2014	4	1	2	0.2					12	41		0.1	0.2	3	0.08	36		SPAP
2015	1	0.1	1	0.01		1	1	16	5	6	4	0.2	0.5	1	0.08	63		SPAP
	12	1	30	14	2	14	0.4	1	5	0.4	1	0.1	1	2	0.19	16		SPAP
1989	40.0	1				5.0		0.6			11.0	0.60		9.9		32.3		283032.5
1989	2.5		1.9		1.3	0.9	6.5	6			32.0	8.70	0.7	5.0	0.2	34.1		283052.5
1989			0.5			2.5		25			21.0	0.30	0.9	1.6	0.2	48		283062.5
2004	0.7		30.0		13.0	22.0	0.2	0.6	2.7	0.2	0.9	0.0	0.1	1.2		28.39	South Africa	3991
2004			0.5			0.3		22.0			12.0	0.60	0.9	3.0	0.2	60.5	Ohio	3547
2009	8.0		0.5			2.5		25.0			21.0	0.30	0.9	1.6	0.2	40		91179

Note:

1. The values under different components are the weight percentage in PM_{2.5}, %; the number under data source represents the code number in speciate_5.0_0
2. SPAP: Database of Source Profiles of Air Pollution (SPAP, <http://www.nkspap.com:9091/>), measured by State Environmental Protection Key Laboratory of Urban Ambient Air Particulate Matter Pollution Prevention and Control & Tianjin Key Laboratory of Urban, Nankai University.

Table TE9 Industrial process (Cement) source profiles from published literatures in China, SPAP and SPECIATE database

Year	SO ₄ ²⁻	NO ₃ ⁻	Cl ⁻	NH ₄ ⁺	Na	K	Mg	Ca	OC	EC	Fe	Mn	Al	Si	Ti	Other	City/Region	Data source
2001	14				1.7	1.4	0.4	36	2	0.3	1.7	0.0	1.2	4.8	0.1	36.4	Hongkong	(Ho et al., 2003)
2006	3	0.3	0.2	0.3	0.2	2.7	0.5	24	3	0.7	3.7	0.1	5	6.2	0.4	49.7	Hangzhou	(Bao et al., 2010)
2014~2015	10	1.8		2.7	0.5	0.8	1.7	11	14	2.1	5.5	0.0	4.6	10.1	0.3	34.9		(Liu et al., 2017)
2014~2015	16	0.7		0.6	0.7	0.5	1.8	12	5	6.2	4.7	0.1	3.1	9.4	0.2	39.2		
		0.4	0.2		0.1	2.3	0.8	59	20	1.9	5.3	0.3	2	5.5	0.4	1.4	Jing-Jin-Ji	
			0.2		0.1	1.1	0.6	64	23	0.6	3.9	0.0	1.3	3.8	0.2	1.2	Jing-Jin-Ji	(Ye et al., 2017)
	0.2	0.5	0.4		0.1	2.1	0.9	52	29	2.2	3.5	0.0	2.2	5.9	0.2	1.2	Jing-Jin-Ji	
		1.2	0.2		0.1	1.8	1.5	68	9		4.3	0.1	3.2	8.2	0.3	1.6	Jing-Jin-Ji	
2017	21	0.7	2.2	4.5	1.2	0.8	1.4	3	2	0.5	3.2	0.1	5.2	11.4		42.8	Wuhan	(Gong and Luo, 2018)
2016	4.9	0.4	0.5	1.6	1.4	1.1	1.5	19.1	4.9	1.9	2.3	0.1	3.5	7.0	0.1	50		SPAP
2016	4	0.3	0.1		0.3	1	1	31	1	5	2	0.03	2	9	0.2	42		SPAP
2017	1	2	1	2		0.4	0.3	15	4	0.2	2	0.04	3	0.3	0.03	69		SPAP
2017	0.5	0.02	0.2	1	0.3	0.5	1	17	10	1	1	0.03	1	2	0.02	66		SPAP
1989	18	0.2	7.8		2.3	5.4	0.2	10	5	0.2	0.9	0.0	4.3	8.4	0.3	36.6		272032.5
1997	0	0.1	0.1	0.0	0.0	0.3	0.1	30	14	0.0	1.7	0.0	0.7	2.8	0.0	49.0	Mexico	4087
1999	38	4.6	3.9	1.2	2.4	21.8	0.0	10	12	1.0	1.1	0.1	0.8	3.1	0.1	0.2	Texas	4333
2002	31	8.9	7.1	2.4	2.3	11.6	0.1	18	13	3.0	1.3	0.1	1.1	4.3	0.1		Texas	4378
2006	18	4.7	3.2	2.4	2.3	7.0	0.1	17	13	3.0	0.7	0.1	1.1	4.3	0.3	23.5		91004
2009	18	4.7	3.1	2.3	2.3	6.9	0.1	17	13	2.9	0.7	0.1	1.1	4.2	0.3	24.4		91127

Note:

1. The values under different components are the weight percentage in PM_{2.5}, %; the number under data source represents the code number in speciate_5.0_0

2. SPAP: Database of Source Profiles of Air Pollution (SPAP, <http://www.nkspap.com:9091/>), measured by State Environmental Protection Key Laboratory of Urban Ambient Air Particulate Matter Pollution Prevention and Control & Tianjin Key Laboratory of Urban, Nankai University.

Table TE10 Transportation sector (Heavy duty gasoline) source profiles from published literatures in China, SPAP and SPECIATE database

Year	SO ₄ ²⁻	NO ₃ ⁻	Cl ⁻	NH ₄ ⁺	Na	K	Mg	Ca	OC	EC	Fe	Mn	Al	Si	Ti	Other	City/Region	Data source
2005~2006	1				0.8	0.3	0.3	2.4	60	24	0.4		0.2	1	0.1	9.7	Tianjin	(Zhang, 2007)
2009	2	0.2		0.6	0.35			0.71	40	22			1	3.1		30.0	Dongying	(Kong, 2012)
2012	6	1.4	1.1	1.8	2	0.9	0.9	1.5	52	24	1		0.2	0.3		7.6	Pearl River Delta	(Feng, 2013)
2012	1	0.7	0.5	0.1	0.7	0.3	0.1	0.9	29	61	0.6					4.7	Hubei	(Zhang et al., 2015)
2012	1	0.6	0.6	0.1	0.6	0.3	0.1	0.6	32	59	0.7					4.0	Hubei	
2014~2015	9	1.9	0.3	2.9	0.6	0.5	0.2	0.8	19	43	0.3		0.1			21.3	Hengshui	
2014~2015	9	2.7	0.6	2.2	0.7	0.6	0.2	0.6	16	40	0.4		0.3			26.9	Hengshui	(Wang et al., 2015)
2014~2015	8	1.9	0.4	4	0.5	0.5	0.3	0.8	20	39	0.3		0.2			24.6	Hengshui	
2015		1.0	0.2					0.2	31.4	19.8	0.1	0.01	0.3	0.8	0.002	46.2		SPAP
2015		1.0	1.0					0.2	41.6	24.4	0.1	0.01	0.4		0.001	31.3		SPAP
1989	5				0.8	0.2	0.9	0.7	21	55	0.6	0.0	1.0	1.6	0.0	13.3	-	322022.5
1989			0.0			0.0		0.1	36	52			0.0	0.0	0.0	11.9	-	322032.5
1990			0.0					0.1	36	52			0.0	0.0	0.0	11.9	-	322072.5
1999	0	0.3	0.3	0.1	0.2	0.1		0.2	33	41	0.1	0.0	0.1	0.6	0.0	23.9	Los Angeles	322082.5

2000	30	0.8	1.4	5.1		0.0		3	16	33	0.1	0.01		0.6	0.2	10.0	Ottawa	4750
2000	1	0.1	0.1	0.1				0	44	46		0.06	0.1	0.5		8.0	Ottawa	4749
2001	1		0.0	0.2	0.1	0.0	0.0	0	25	63	0.1		0.0	0.5		10.4	California	4860
2005	3	0.2	0.0	1.0		0.0	0.0	0	15	70	0.1	0.00		0.2		10.1	Los Angeles	4972
2005	2	0.3	0.1	0.4	0.0	0.0	0.0	1.2	62	30	0.3	0.0	0.0	0.0		3.3	Los Angeles	4978
2008	40				0.9	0.0	0.1	0.4	49	7	0.4	0.01	0.1	0.1	0.0	2.4		5679
2012	1	15.9		1.2	0.1	0.0		0.4	52	14	0.2	0.01	0.1	0.1	0.0	15.2		95334

Note:

1. The values under different components are the weight percentage in PM_{2.5}, %; the number under data source represents the code number in speciate_5.0_0
2. SPAP: Database of Source Profiles of Air Pollution (SPAP, <http://www.nkspap.com:9091/>), measured by State Environmental Protection Key Laboratory of Urban Ambient Air Particulate Matter Pollution Prevention and Control & Tianjin Key Laboratory of Urban, Nankai University.

Table TE11 Transportation sector (Light diesel) source profiles from published literatures in China, SPAP and SPECIATE database

Year	SO ₄ ²⁻	NO ₃ ⁻	Cl ⁻	NH ₄ ⁺	Na	K	Mg	Ca	OC	EC	Fe	Mn	Al	Si	Ti	Other	City/Region	Data source
2002	5.9	1.0	0.2	0.5	0.0	0.0	0.0	0.0	10	21	0.2	0.0	0.0	0.0	0.0		Yantai	(Cui et al., 2017)
2009	15	1.2		1.8	0.9				38	6			1.0	2.5			Dongying	(Kong, 2012)
2009~2015	0.1	1.9	0.3	0.2	0.3	0.0	0.0	0.2	36	24	0.1	0.0	0.2	0.6	0.0		Fen-Wei plains	(Hao et al., 2019)
2013~2014	1.1	0.1	0.3	0.0		0.1		0.1	16	24	1.2	0.0	0.7	0.6	0.2		-	(Liu et al., 2018)
2015	0.3	3.3	0.2		0.0	0.00	0.1	0.4	32	19	0.3		0.2	0.7	0.4	44		SPAP
	3.0	2.3	0.8	1.5	0.4	0.1	0.4	0.5	34.6	19.2	0.2	0.04	0.3	0.8	0.1	36		SPAP
1987	3.2		0.1	0.6	0.1			0.1	49	43	0.0			0.3	0.0		California	3463

1988	1.4	0.1	0.1	0.3		0.0		0.2	18	78	0.6		0.4			Denver	3219
1989	2.4	0.3	1.6	0.9		0.0		0.2	40	33	0.2	0.0	0.2	0.5		Phoenix	3518
1996	0.4	0.2	0.0		0.0	0.0	0.0	0.1	42	48	0.1		0.0	0.4		Colorado	3960
1997	0.4	0.2	0.1		0.1		0.1	0.1	19	75	0.0		0.0	0.5		Colorado	3878
1998	3.2	2.8	0.6	1.4	0.4	0.8		0.4	52	37	0.3	0.0	0.5	0.8	0.0	Mexico	4014
2001	1.9		0.2	0.5	0.0	0.0	0.2	0.3	37	43	0.2		0.1			California	4842
2007	5.3	1.3	0.4	1.7	0.3	0.3	0.1	0.6	35	46	0.3		0.1	0.3	0.0		8994

Note:

1. The values under different components are the weight percentage in PM_{2.5}, %; the number under data source represents the code number in speciate_5.0_0
2. SPAP: Database of Source Profiles of Air Pollution (SPAP, <http://www.nkspap.com:9091/>), measured by State Environmental Protection Key Laboratory of Urban Ambient Air Particulate Matter Pollution Prevention and Control & Tianjin Key Laboratory of Urban, Nankai University.

Table TE12 Transportation sector (Light duty gasoline) source profiles from published literatures in China, SPAP and SPECIATE database

Year	SO ₄ ²⁻	NO ₃ ⁻	Cl ⁻	NH ₄ ⁺	Na	K	Mg	Ca	OC	EC	Fe	Mn	Al	Si	Ti	Other	City/Region	Data source
2009~2015	0.1	2.0	0.3		0.3	0.0	0.1	0.4	48	6	0.5	0.5	0.4	0.4		41.0	Fen-Wei plains	(Hao et al., 2019)
2010	3.9	1.8	0.8		1.1	0.2	0.7	7.8	39	29	2.9	0.1	4.3	4.2	0.1	4.2	Xining	(Kong, 2012)
2010	9.7	1.7	2.4		2.3	1.2	2.8	6.6	29	18	1.6	0.4	8.6	4.9	0.2	10.8	Xining	
2013		1.5	5.4		3.3	0.1	0.4	2.5	54	21	0.6	0.1	0.5			10.7	Xiamen	(Zhang et al., 2016)
2017	5	6	4	2	1	1	0.2	1	33	34	0.4	1	1		0.02	14		SPAP
2017	2	5	5	5	0.5	0.3	0.4	0.4	25	38	0.5	0.5	1		0.02	16		SPAP
	1	3	1	4	0.2	0.1	0.2	1	54	12	0.5	0.5	0.5	0.4	0.01	23		SPAP
2015	0.03	2	0.2		0.0002	0.002	0.01	0.3	69	1	0.1	0.2	0.2	0.2	0.002	26		SPAP

2015	0.1	2	0.2		0.02	0.004	0.01	0.2	77	2	0.1	0.2	0.2	0.2	0.003	18		SPAP
1989	17		1.8			0.01		0.1	24	6	0.1	0.0	0.1	0.2		50.8	-	312302.5
1990			0.3			0.05		0.1	31	15	0.1	1.0	0.6	0.8	0.0	51.1	-	311062.5
1999	3.6	1.8	2.5		1.5				50	23	0.2		0.1	0.0	0.0	17.3	-	311072.5
1999	0.5	0.6	0.9		0.5	0.1			66	8	0.8	0.9	0.7	0.4	0.0	20.7	-	311082.5
2001	9.9	1.1	1.3	5.1	0.1	0.0	0.2	0.1	48	14	0.3	0.0	0.1	3.1	0.0	16.8	California	4895
2004	1.1	0.0			0.8	0.0	0.1	2.1	73	18	0.1	0.0	0.0	0.6	0.0	4.1	Kansas	5570
2005	7.4	0.1			0.1	0.0	0.0	0.2	66	12		0.0	0.1	0.3	0.0	13.8	Kansas	5592
2010	7.2	0.3	0.1	2.8		0.1	0.1	1.4	56	14	1.8	0.0	0.3	0.3	0.0	15.6		8993

Note:

1. The values under different components are the weight percentage in PM_{2.5}, %; the number under data source represents the code number in speciate_5.0_0
2. SPAP: Database of Source Profiles of Air Pollution (SPAP, <http://www.nkspap.com:9091/>), measured by State Environmental Protection Key Laboratory of Urban Ambient Air Particulate Matter Pollution Prevention and Control & Tianjin Key Laboratory of Urban, Nankai University.

Table TE13 Residential coal combustion source profiles from published literatures in China, SPAP and SPECIATE database

Year	SO ₄ ²⁻	NO ₃ ⁻	Cl ⁻	NH ₄ ⁺	Na	K	Mg	Ca	OC	EC	Fe	Mn	Al	Si	Ti	Other	City/Region	Data source
2004			10.5		1.3	17.4		0.1	3		0.1		0.1	0.3		67.2	Yangquan	(Ge et al., 2004)
2004						1.2	0.3	0.6	12	4	0.8		1.5	3.4	0.1	76.4	Yangquan	
2009	31	0.8	5.6	0.5	2	10.4	0.1	0.3	36		0.4		0.2			12.4	Dongying	(Kong, 2012)
2009	8	0.6	0.7		1.8	1.3	0.9	2.4	69	6	2.1	0.1	1.9			5.6	Dongying	
2012~2014					0.8	1.5	1.1	1.0	18	8	7.8		11.3	25.4	2.2	23.3	Guiyang	(Wang et al., 2016)
2016~2017	17	0.4	1.9	2.1	0.8	0.4			49							28.0	Xian	(Dai et al., 2019)

2016~2017	29	1.1	1.1	9.9	1.8	0.1	0.2		32	5			0.1	19.5	Xian		
2017~2018	40	0.3	0.9	18	1.6	0.8	0.02	0.6	3	0.4	0.1		0.2	0.4	33.7	SPAP	
2017	28	1.2	2	16	4.1	0.5	0.2	2.2	10	0.9	0.3		1.7	4.8	28.1	SPAP	
2017	31	0.4	20.1	20	1.5	1	0.1	0.8	3	0.3	0.2		0.1	0.4	21.1	SPAP	
	21.7	0.5	2.1	6.0	2.2	1.8	0.2	0.9	23.3	5.8	0.8	0.02	1.5	2.1	0.2	30.9	SPAP
1995	7	0.8	0.3	3.1		1.7	0.1	0.8	45	33	0.2		0.2	0.2	8.4	Colorado	3758
1995	2	0.2	0.1	1		0.1			76	21			0.1			Colorado	3759
1995	3	0.3	0.2	1		0.5		0.2	69	26	0.1		0.1	0.1		Colorado	3761
1997	1	0.2	0.1						56	19			0.1		23.3	South Africa	4007
2009	3	0.3	0.1	1.4		0.5	0.3	1.2	45	24	0.9		0.7	0.7	23.0	Colorado	91155

Note:

1. The values under different components are the weight percentage in PM_{2.5}, %; the number under data source represents the code number in speciate_5.0_0
2. SPAP: Database of Source Profiles of Air Pollution (SPAP, <http://www.nkspap.com:9091/>), measured by State Environmental Protection Key Laboratory of Urban Ambient Air Particulate Matter Pollution Prevention and Control & Tianjin Key Laboratory of Urban, Nankai University.

TE6

Article structure: Eq. (1) and its discussion should be part of Section 2.2. Please consider shortening the titles of Sections 3 to 5.

Thank you for your advice. We have rewritten the section 2.2, added discussion on the Coefficient Divergence (CD) values between different source profiles, and shorten the titles of Section 3 to 5. The detail description are as follows:

The CD values of coal-fired power plant (PP), industrial process (IN), transportation sector (TR), residential coal combustion (RE) source profile between SPAPPC and SPECIATE database are 0.64 ± 0.10 (0.34~0.92), 0.72 ± 0.09 (0.45~0.94), 0.69 ± 0.09 (0.33~0.86), 0.75 ± 0.10 (0.58~0.91), respectively; The CD values between different sources are 0.78 ± 0.10 (0.32~1.00), which show obvious differences among PM_{2.5} source profiles in source category. Detailed information is shown in Fig. TE5~TE8 (Fig. S2~S6 in our supplementary material).

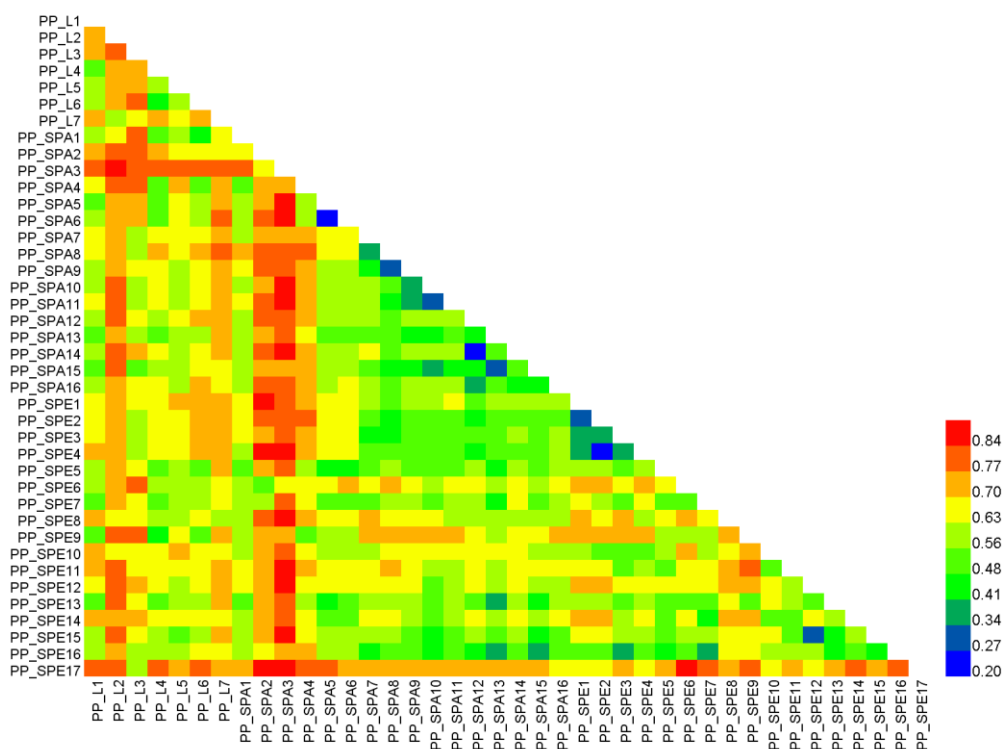


Fig. TE5 The coefficient divergence values for PP source profiles

Note: Power plant source profiles from published literatures in China (PP_L), SPAP (PP_SPA) and

SPECIATE database (PP_SPE). Numbers represent source profile sequence number.

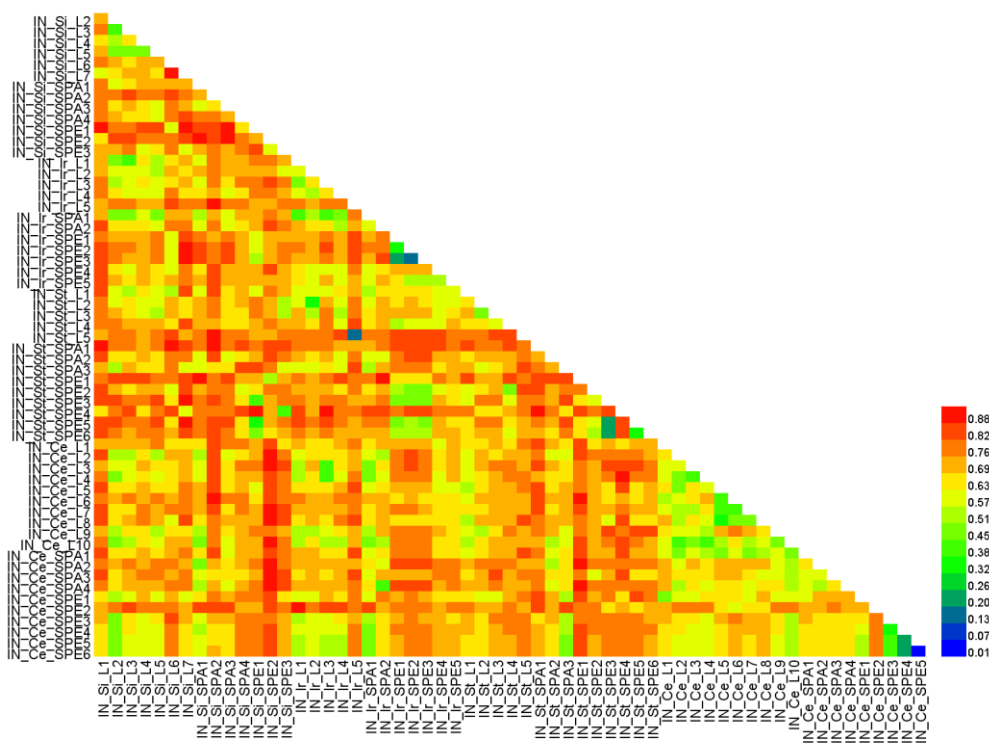


Fig. TE6 The coefficient divergence values for IN source profiles.

Note: Industrial process (sintering) source profiles from published literatures (IN_Si_L) in China, SPAP (IN_Si_SPA) and SPECIATE database (IN_Si_SPE); Industrial process (iron-making) source profiles from published literatures in China (IN_Ir_L), SPAP (IN_Ir_SPA) and SPECIATE database (IN_Ir_SPE); Industrial process (steelmaking) source profiles from published literatures in China (IN_St_L), SPAP (IN_St_SPA) and SPECIATE (IN_St_SPE) database; Industrial process (Cement) source profiles from published literatures in China (IN_Ce_L), SPAP (IN_Ce_SPA) and SPECIATE database (IN_Ce_SPE). Numbers represent source profile sequence number.

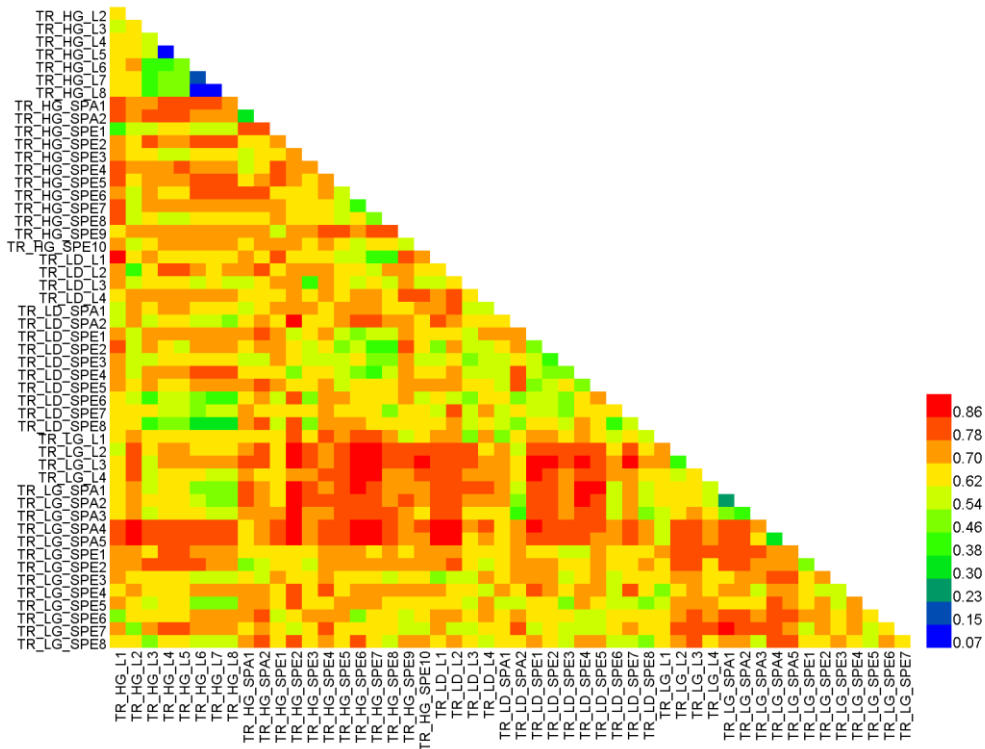


Fig. TE7 The coefficient divergence values for TR source profiles

Note: Transportation sector (Heavy duty gasoline) source profiles from published literatures in China (TR_HG_L), SPAP (TR_HG_SPA) and SPECIATE (TR_HG_SPE) database. Transportation sector (Light diesel) source profiles from published literatures in China (TR_LD_L), SPAP (TR_LD_SPA) and SPECIATE (TR_LD_SPE) database. Transportation sector (Light duty gasoline) source profiles from published literatures in China (TR_LG_L), SPAP (TR_LG_SPA) and SPECIATE (TR_LG_SPE) database. Numbers represent source profile sequence number.

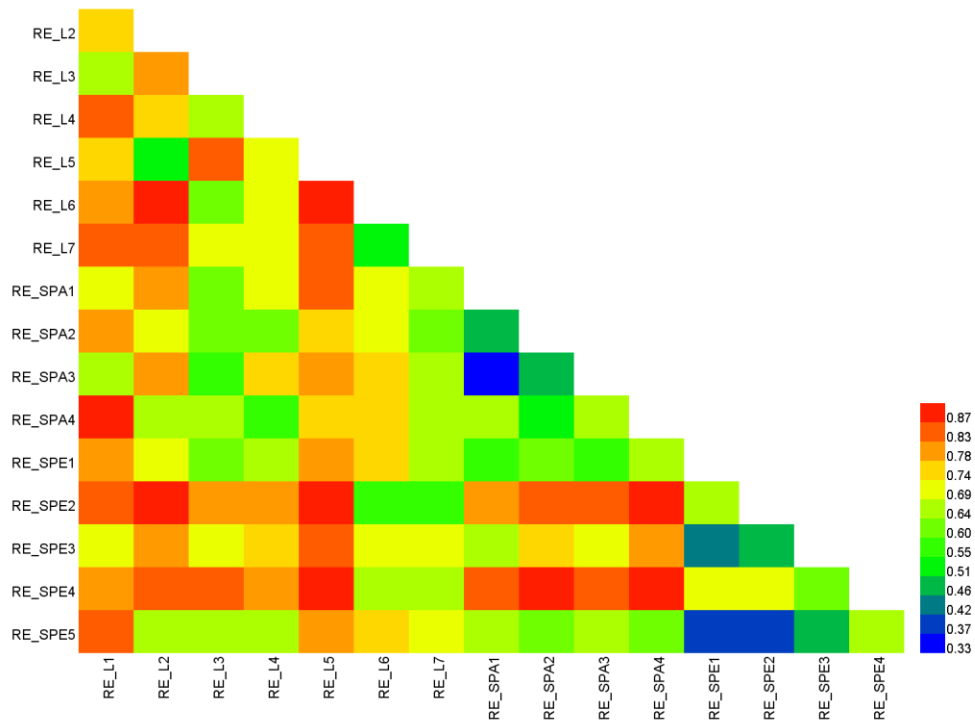


Fig. TE8 The coefficient divergence values for RE source profiles

Note: Residential coal combustion source profiles from published literatures in China (RE_L), SPAP (RE_SPA) and SPECIATE (RE_SPE) database. Numbers represent source profile sequence number.

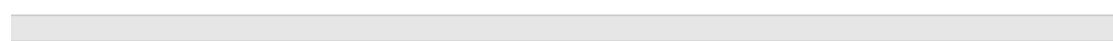
We insert eq.(1) in section 2.2, which is shown in the screenshot 5 below.

Screenshot 5:

204 To determine the similarity between the two groups of source profiles, Coefficient
 205 Divergence (CD) is calculated using the following formula (Wongphatarakul et al.,
 206 1998):

$$CD_{jk} = \sqrt{\frac{1}{p} \sum_{i=1}^p \left(\frac{x_{ij} - x_{ik}}{x_{ij} + x_{ik}} \right)^2} \quad \text{..... (1)}$$

208 Where CD_{jk} is the coefficient of divergence of source profile j and k , p was the
 209 number of chemical components in source profile, x_{ij} is the weight percentage for
 210 chemical component i in source profile j , x_{ik} is the weight percentage for i in source
 211 profile k (%). The CD value is in the range of 0 to 1, if the two source profiles are
 212 similar, the value of CD is close to 0; if the two are very different, the value was close



213 to 1.

The titles of Section 3-5 are shorted as:

Section 3- Is there an impact of variation of source profile on the simulation results?

Section 4- How much does it impact?

Section 5- How does the impact work?

TE7

Line 281: Specify which station location is used.

Thank you for your comments. We have revised the original sentence as “We selected one air quality monitoring station (Site 8 as the selected station here and any site could be available) to explore the effect of emission source chemical profiles on simulated PM_{2.5} components, then used the left 9 sites to further illustrate the conclusions suggested.” The modified text is shown in screenshot 6 below:

Screenshot 6:

325 ~~domain.~~We selected one air quality monitoring station (Site 8; as the selected station
326 here and any one site could be available) to explore the effect of emission source
327 chemical profiles on simulated PM_{2.5} components~~study the influence of PM_{2.5} source~~
328 ~~profile on numerical simulation of PM_{2.5}-bound components and to explore the relevant~~
329 ~~laws in the atmosphere~~, then used the left 9 sites to further illustrate the conclusions
330 suggested. ↵

TE8

Please clearly define in the main document what the numerical values represent, i.e., where appropriate, mention that you are discussing mean values and indicate the averaging period (e.g., Fig. 6, Eq. (2) etc.).

Thank you for your comments. The numerical values of Fig.6 and Eq. (2) are the mean values from Oct. 1 to Oct. 30 in 2018. We have clearly defined what the numerical values represent in the revised manuscript. The details are shown as following screenshots 7-9.

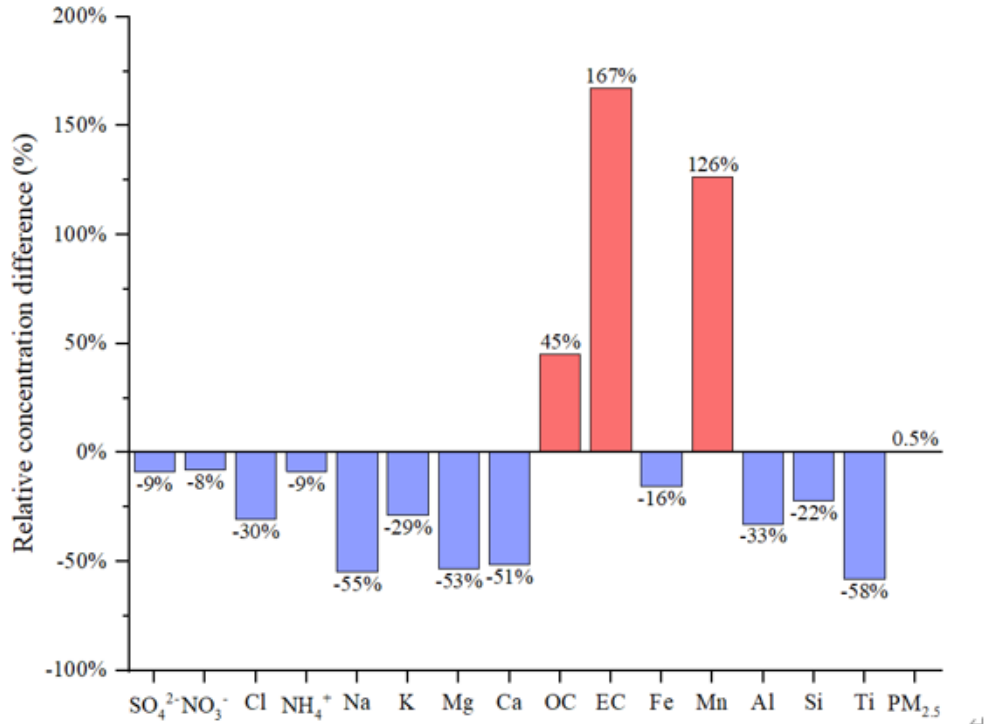
Screenshot 7:

164 data archived at National Center for Atmospheric Research (NCAR). In addition,
165 surface and upper air observations obtained from NCAR were used to further refine the
166 analysis data. The modeling was conducted from Oct. 1 to Oct.30 in 2018. ~~The and~~
167 major configurations we used in CMAQ were illuminated as follows: Gas-phase

Screenshot 8:

331 The simulation results for PM_{2.5} species under CMAQ_SPA and CMAQ_SPE
332 cases also showed big differences (as shown in Fig. 6-3 and Table S13), ~~in which the~~
333 ~~The~~ largest difference in average simulated concentration was EC with CAMQ_SPE
334 giving higher by 167% than CMAQ_SPA; For OC and Mn, higher values were also
335 given by CMAQ_SPE than by CMAQ_SPA (45% and 126% on average, respectively);
336 For the ~~remaining-other~~ components of concern, the simulated concentration by
337 CMAQ_SPE was lower than CMAQ_SPA with Ti (58%), Na (55%), Mg (53%), Ca
338 (51%), Al (33%), Cl (30%), K (29%), Si (22%), Fe (16%), NH₄⁺ (9%), SO₄²⁻ (9%), NO₃⁻
339 (8%), separately. While the simulated PM_{2.5} concentrations under the two cases were
340 quite close. The influence of source profile variation on the simulated PM_{2.5}
341 concentration was not significant, but the influence on the simulation of chemical
342 components in PM_{2.5} could not be ignored.↵

Screenshot 9:



344

345 Fig. 6-3 The percentage relative concentration difference of average simulated concentration result

18

346 (PM_{2.5} and its components) between CMAQ_SPE and CAMQ_SPA (relative to CAMQ_SPA)
 347 during simulation period; PM_{2.5} source profiles from SPAPPC and SPECIATE database were
 348 applied in emission inventory for simulating PM_{2.5} and its components used to create speciated
 349 emission inventories for CMAQ, corresponding to case CMAQ_SPA and CMAQ_SPE, respectively.

TE9

Fig. 6: Clarify the y-axis label (e.g., "Relative concentration difference")

Thank you for your advice. We have revised Fig. 6 in the manuscript, as shown below (Fig. TE9).

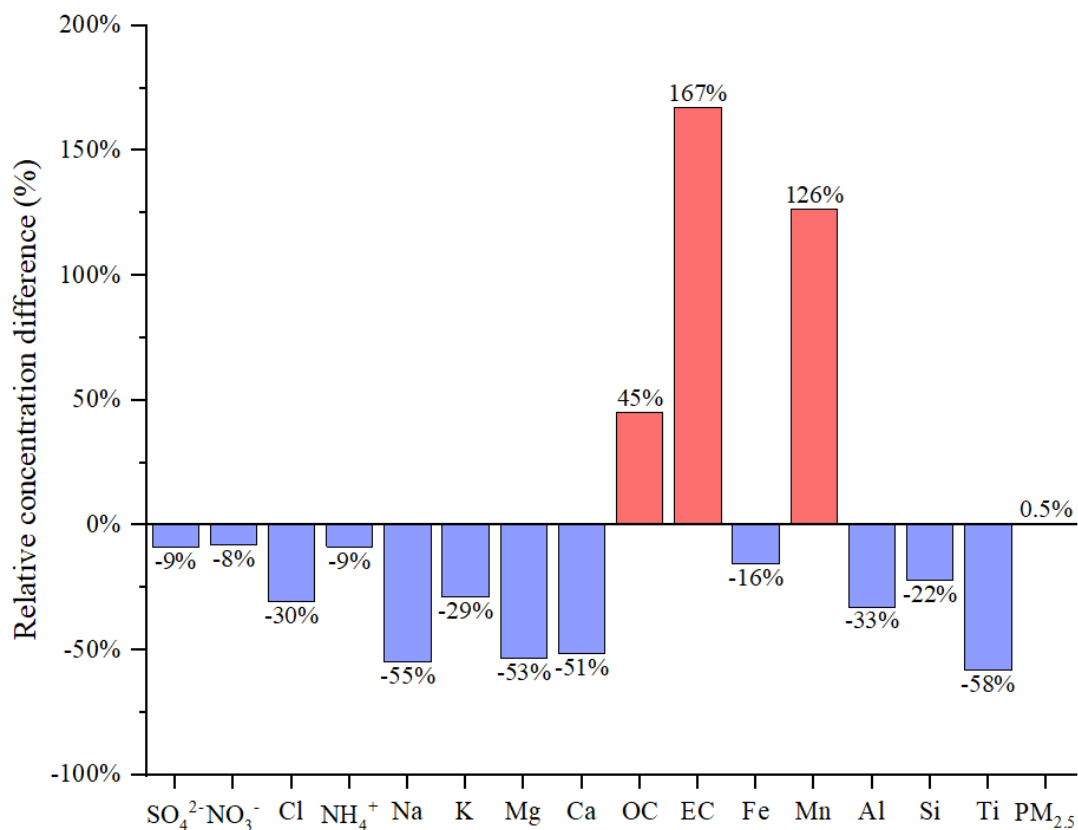


Fig. TE9 The relative concentration difference of average simulated results (PM_{2.5} and its components) between CMAQ_SPE and CAMQ_SPA (relative to CAMQ_SPA) during simulation period; PM_{2.5} source profiles from SPAPPC and SPECIATE database were used to create speciated emission inventories for CMAQ, corresponding to case CMAQ_SPA and CMAQ_SPE, respectively.

TE10

Fig. 7 and Table 1: Please define SNA in the captions.

We have defined SNA in the captions, details as follows (highlighted in yellow):

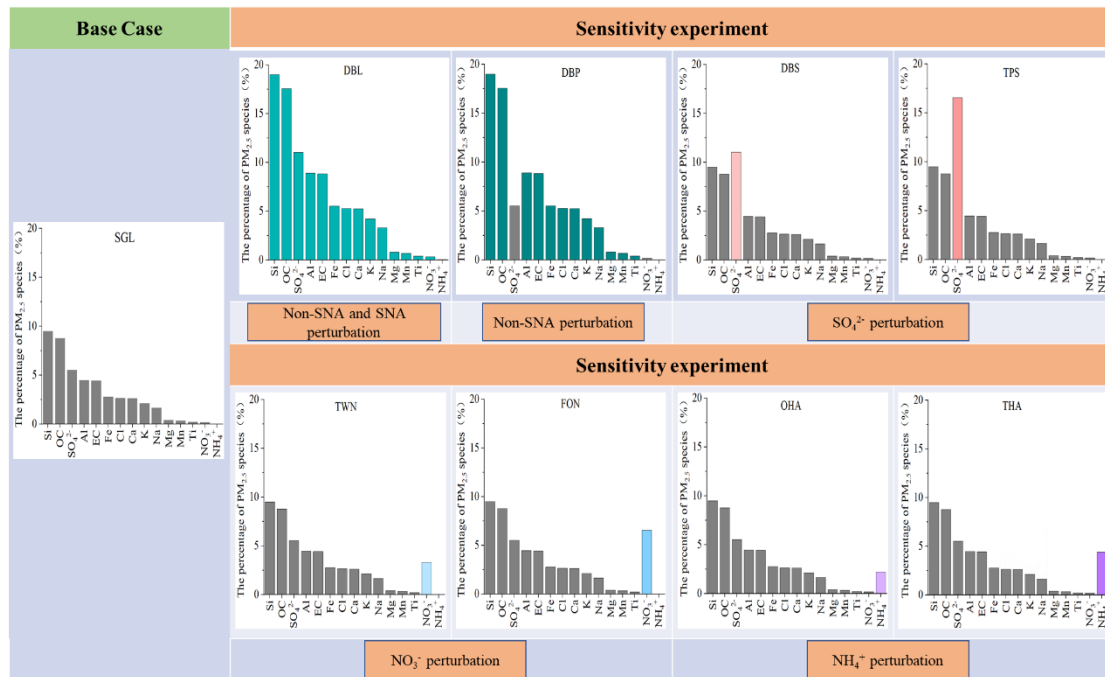


Fig. TE10 The general roadmap of sensitivity tests (The histogram in each case were the speciation profile in CTMs; SNA represent SO_4^{2-} , NO_3^- , and NH_4^+ , Non-SNA represent other components in $\text{PM}_{2.5}$).

Table TE14 The content of sensitivity experiment cases

Cases	Description
Case DBL: add perturbation to Non-SNA and SNA	The percentage of all the listed components in the source profile of base case (SGL) were doubled, and the proportion of unlisted components (Other) decreased to 9%.
Case DBP: add perturbation to Non-SNA	The percentages of non-SNA were doubled and SNA (SO_4^{2-} , NO_3^- , NH_4^+) species stayed the same with that in SGL (the cumulative percentage of listed species was 85.3%), the proportion of unlisted components decreased to 14.7%.
Case DBS and TPS: add perturbation to SO_4^{2-}	The percentage of SO_4^{2-} was doubled (11%, DBS, represented Double Sulfate), tripled (16.5%, TPS, represented Triple Sulfate) and the other listed 14 species stayed the same with that in SGL (the cumulative percentage of listed species was 51% and 57%, respectively), the proportion of unlisted components decreased to 49% and 43%.
Case TWN and FON: add perturbation to NO_3^-	The NO_3^- content was raised up to 20 times (3.3%, TWN) and 40 times (6.6%, FON) of that in SGL (0.16%), the other 14

species stayed the same with SGL (the cumulative percentage of listed species was 48.6% and 51.9%, respectively), the proportion of unlisted components decreased to 51.4% and 48.1%.

Case OHA and THA:
add perturbation to NH_4^+

The NH_4^+ content was raised up to 100 times (2.2%, OHA), 200 times (4.4%, THA) of that in SGL (0.02%), the other 14 species stayed the same with SGL (the cumulative percentage of listed species was 47.7% and 49.9%, respectively), the proportion of unlisted components decreased to 52.3% and 50.1%.

Note:

1. SNA represent SO_4^{2-} , NO_3^- , and NH_4^+ , Non-SNA represent other components in $\text{PM}_{2.5}$.

2. The listed components contain Al, Ca, Cl, EC, Fe, K, Mg, Mn, Na, OC, Si, Ti, NH_4^+ , NO_3^- and SO_4^{2-} , unlisted components are classified as Other.

3. The source profiles in all cases listed in the table were calculated based on the base case SGL.

In the design of simulation cases, the reason why the disturbance amplitude of NH_4^+ and NO_3^- were significantly higher than that of other components such as SO_4^{2-} and Non-SNA, was because the percentages of NH_4^+ and NO_3^- in the base source profile (SGL, based on the chemical composition of code 000002.5 in the EPA Speciate_5.0_0 database) were very low, while the percentage of NH_4^+ and NO_3^- in SPAPPC exhibited in section 2.2 were orders of magnitude higher than those in SGL.

TE11

Table 2: The labels "Case S1" to "Case S4" are not used elsewhere, please reconsider the labelling. The choice of the factors used to enhance the components should be discussed and motivated in the main text. Note that to qualify as a model experiment description paper the article "should include the discussion of why particular choices were made in the experiment design" (cf. https://www.geoscientific-model-development.net/about/manuscript_types.html).

Thank you for your advice. We relabeled the sensitivity experiment cases to ensure consistency. To address the editor's comment, please see the point-by-point response as follows:

In Table 2, Case S1 represents add perturbation to Non-SNA (components other than SO_4^{2-} , NO_3^- , and NH_4^+ in $\text{PM}_{2.5}$ emission profiles), Case S2 stands for add

perturbation to SO_4^{2-} , Case S3-perturbation to NO_3^- , Case S4-add perturbation to NH_4^+ . In order to ensure consistency, we relabeled “Case S1” as Case DBP, “Case S2” is subdivided into Case DBS and TPS, “Case S3” as Case TWN and FON, “Case S4” as OHA and THA.

The first column (“Cases” column) in Table 2 represents the simulation cases (base case and sensitivity experiments group). The column “ R_1 ”, “ R_2 ” and “ R_3 ” represent the “total sulfate ratio”, “crustal species and sodium ratio” and “crustal species ratio” respectively. R_1 's value is determined by molar concentration of NH_4^+ , Ca^{2+} , K^+ , Mg^{2+} , Na^+ and SO_4^{2-} , R_2 is controlled by Ca^{2+} , K^+ , Mg^{2+} , Na^+ and SO_4^{2-} , and R_3 is influenced by Ca^{2+} , K^+ , Mg^{2+} and SO_4^{2-} . The last column (“Solid phase species”) is the aerosol composition. In CMAQ model, the aerosol thermodynamic equilibrium process is carried out according to ISORROPIA II (thermodynamic equilibrium model), including a SO_4^{2-} - NO_3^- - Cl^- - NH_4^+ - Na^+ - K^+ - Mg^{2+} - Ca^{2+} - H_2O system. The number of species and equilibrium reactions is determined by the relative abundance of NH_3 , Na, Ca, K, Mg, HNO_3 , HCl , H_2SO_4 , as well as the ambient relative humidity and temperature. Guided by the value of R_1 , R_2 and R_3 , 5 aerosol composition regimes in ISORROPIA are defined, detailed rules are shown in the following Table TE15.

Table TE15 Five aerosol types in ISORROPIA and corresponding R value

R_1	R_2	R_3	Aerosol type	Solid phase
$R_1 < 1$	any value	any value	Sulfate Rich (free acid)	NaHSO_4 , NH_4HSO_4 , KHSO_4 , CaSO_4
$1 \leq R_1 \leq 2$	any value	any value	Sulfate Rich	NaHSO_4 , NH_4HSO_4 , Na_2SO_4 , $(\text{NH}_4)_2\text{SO}_4$, $(\text{NH}_4)_3\text{H}(\text{SO}_4)_2$, CaSO_4 , KHSO_4 , K_2SO_4 , MgSO_4
$R_1 \geq 2$	$R_2 < 2$	any value	Sulfate Poor, Crustal & Sodium Poor	Na_2SO_4 , $(\text{NH}_4)_2\text{SO}_4$, NH_4NO_3 , NH_4Cl , CaSO_4 , K_2SO_4 , MgSO_4
$R_1 \geq 2$	$R_2 \geq 2$	$R_3 < 2$	Sulfate Poor, Crustal & Sodium Rich,	Na_2SO_4 , NaNO_3 , NaCl , NH_4NO_3 , NH_4Cl , CaSO_4 , K_2SO_4 , MgSO_4

Crustal Poor

$R_1 \geq 2$	$R_2 \geq 2$	$R_3 > 2$	Sulfate Poor, Crustal & Sodium Rich, Crustal Rich	NaNO ₃ , NaCl, NH ₄ NO ₃ , NH ₄ Cl, CaSO ₄ , K ₂ SO ₄ , MgSO ₄ , Ca(NO ₃) ₂ , CaCl ₂ , Mg(NO ₃) ₂ , MgCl ₂ , KNO ₃ , KCl
--------------	--------------	-----------	---	---

Source: Fountoukis and Nenes, 2007

By summarizing the source profile through the published literatures and existing source profile databases, we found that the main components and their contents of different PM_{2.5} sources were significantly different. Source profile, i.e. species allocation in emission sources, is used to create speciated emission inventories for CTMs. In order to explore the sensitivity of simulated PM_{2.5} components to changes in source profile, different simulation scenarios were designed.

Step1: Provide perturbation range for experiment cases based on the variation range of components' measured values

The perturbation rules must be followed: a) perturbation on the percentage of each component in source profile fell within the variation range of its measured value described in section 2.2; b) The sum of the percentage of Non-SNA, SNA and Other components in PM_{2.5} source profile was 100%. The design idea is shown in Figure TE11.

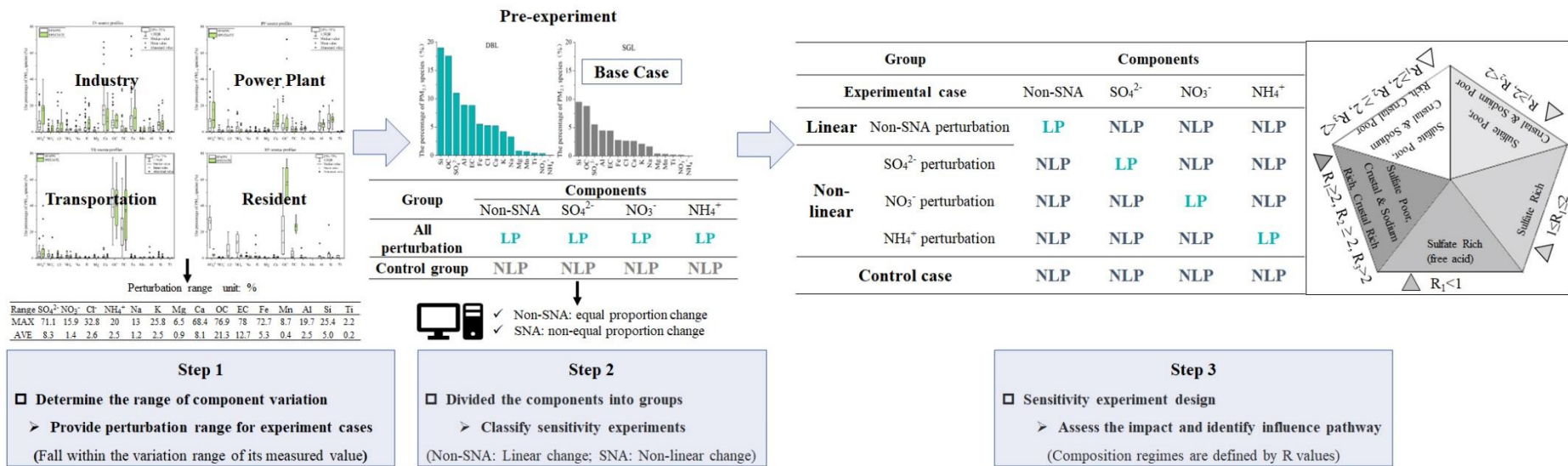
Step2: Classify the experiment cases

Through the pre-experiment, we found the impact pattern for SNA (SO₄²⁻, NO₃⁻, and NH₄⁺) and Non-SNA were obviously different: When we perturb the percentage of all the components except “other” in the source profile, the simulated concentrations of Non-SNA were equal proportion change (Linear), while the simulated concentration of NO₃⁻, SO₄²⁻ and NH₄⁺ were not equal proportion change (Non-linear). Therefore, we divided the components in the source profile into four groups (Non-SNA, SO₄²⁻, NO₃⁻, and NH₄⁺), then sensitivity experiment of perturbation on Non-SNA, perturbation on SO₄²⁻, perturbation on NO₃⁻, and perturbation on NH₄⁺ were determined.

Step 3: Assess the impact and identify the influence pathway

We try to answer (1) How much does the variation of source profile impact on the

simulation of PM_{2.5} chemical components? (2) How does the impact work? We propose the sensitivity coefficient as evaluation index to quantify the impact in each sensitivity experiment. And calculate each R's value in different cases; Base on their values, the prior composition and phase state of species are determined (The major species potentially present are determined by the value of R₁, R₂ and R₃, Table TE15 above). Then base on the perspective of potential composition and phase state of aerosols, chemical reaction priority and multicomponent chemical balance in thermodynamic equilibrium system to explore how does the variation of source profile impact on the simulated chemical components.



Note: SNA represent SO₄²⁻, NO₃⁻, and NH₄⁺, Non-SNA represent other components in PM_{2.5}; LP: Load perturbation; NLP: Not load perturbation

Fig. TE11 The sketch of sensitivity experiment design idea

In order to illustrate this issue more clearly, we have made the following revision in main text and supplementary material (screenshots 10-12 below):

Screenshot 10:

363

Table 1 The content of sensitivity experiment cases

Experiment Cases	Description ³
Case S0 (DBL): add perturbation to Non-SNA and SNA ¹	The percentage of all the listed components in the source profile of base case (SGL) were doubled, and the proportion of unlisted components (Other) ² decreased to 9%.
Case S1 (DBP): add perturbation to Non-SNA	The percentages of non-SNA were doubled and SNA(SO ₄ ²⁻ , NO ₃ ⁻ , NH ₄ ⁺) species stayed the same with that in SGL (the cumulative percentage of listed species was 85.3%), the proportion of unlisted components decreased to 14.7%.
Case S2 (DBS and TPS): add perturbation to SO ₄ ²⁻	The percentage of SO ₄ ²⁻ was doubled (11%, DBS, represented Double Sulfate), tripled (16.5%, TPS, represented Triple Sulfate) and the other listed 14 species stayed the same with that in SGL (the cumulative percentage of listed species was 51% and 57%, respectively), the proportion of unlisted components decreased to 49% and 43%.
Case S3 (TWN and FON): add perturbation to NO ₃ ⁻	The NO ₃ ⁻ content was raised up to 20 times (3.3%, TWN) and 40 times (6.6%, FON) of that in SGL (0.16%), the other 14 species stayed the same with SGL (the cumulative percentage of listed species was 48.6% and 51.9%, respectively), the proportion of unlisted components decreased to 51.4% and 48.1%.

19

Case S4 (OHA and THA): add perturbation to NH ₄ ⁺	The NH ₄ ⁺ content was raised up to 100 times (2.2%, OHA), 200 times (4.4%, THA) of that in SGL (0.02%), the other 14 species stayed the same with SGL (the cumulative percentage of listed species was 47.7% and 49.9%, respectively), the proportion of unlisted components decreased to 52.3% and 50.1%.
---	---

Note:

1. SNA represent SO₄²⁻, NO₃⁻, and NH₄⁺, Non-SNA represent other components in PM_{2.5}.

2. The listed components contain Al, Ca, Cl, EC, Fe, K, Mg, Mn, Na, OC, Si, Ti, NH₄⁺, NO₃⁻ and SO₄²⁻, unlisted components are classified as Other.

3. The source profiles in all cases listed in the table were calculated based on the base case SGL. In the design of simulation cases, the reason why the disturbance amplitude of NH₄⁺ and NO₃⁻ were significantly higher than that of other components such as SO₄²⁻ and Non-SNA, was because the percentages of NH₄⁺ and NO₃⁻ in the base source profile (SGL, based on the chemical composition of code 000002.5 in the EPA Speciate_5.0_0 database) were very low, while the percentage of NH₄⁺ and NO₃⁻ in SPAPPC exhibited in section 2.2 were orders of magnitude higher than those in SGL.

Screenshot 11:

381 SNA were obviously different. Therefore, we divided the components in the source

20

382 profile into two groups (Non-SNA and SNA) and designed a series of sensitivity tests
383 listed in next section to further explore how species allocation of PM_{2.5} in emission
384 sources ~~of CTMs would~~ affect the simulation results. The sketch of sensitivity
385 experiment design idea is shown in Figure S7.

Screenshot 12:

510 insufficient sodium, sulfuric acid would react with ammonia. Based on these
511 assumptions, the ISORROPIA model introduced the following three judgment
512 parameters (R_1 , R_2 and R_3 ~~were calculated by the following formulas~~) to determine the
513 simulation subsystems. these parameters are calculated by the following formulas:

$$514 \quad R_1 = \frac{[\text{NH}_4^+] + [\text{Ca}^{2+}] + [\text{K}^+] + [\text{Mg}^{2+}] + [\text{Na}^+]}{[\text{SO}_4^{2-}]} \dots\dots\dots (3)$$

$$515 \quad R_2 = \frac{[\text{Ca}^{2+}] + [\text{K}^+] + [\text{Mg}^{2+}] + [\text{Na}^+]}{[\text{SO}_4^{2-}]} \dots\dots\dots (4)$$

$$516 \quad R_3 = \frac{[\text{Ca}^{2+}] + [\text{K}^+] + [\text{Mg}^{2+}]}{[\text{SO}_4^{2-}]} \dots\dots\dots (5)$$

517 Where [X] denotes molar concentration of component ($\text{mol}\cdot\text{m}^{-3}$). R_1 , R_2 and R_3
518 are termed as “total sulfate ratio”, “crustal species and sodium ratio” and “crustal
519 species ratio” respectively. The number of species and equilibrium reactions are
520 determined by the relative abundance of NH_3 , Na, Ca, K, Mg, HNO_3 , HCl, H_2SO_4 , as
521 well as the ambient relative humidity and temperature. Guided by the value of R_1 , R_2
522 and R_3 , 5 aerosol composition regimes in ISORROPIA are defined. (Detail rules are
523 shown in Table S27).

TE12

Line 374 and Fig. 8: The negative sensitivity coefficient of NH_4^+ needs further

explanation. For all other stations the corresponding value is positive (Table S14). Moreover, according to lines 326, NH_4^+ increased while $\text{PM}_{2.5}$ did not change much, so a negative delta is surprising.

We are extremely sorry for this **typo error**. The values of NH_4^+ in DBL case are negative. Line 374 and Table S14 have been corrected, and original simulation results are provided for supplementary illustration (TE16 as follow).

Table TE16 The sensitivity coefficients (δ) of simulated components in case DBL at different monitoring sites

Components	δ_1	δ_2	δ_3	δ_4	δ_5	δ_6	δ_7	δ_9	δ_{10}
Al	0.20	0.32	0.39	0.33	0.45	0.44	0.54	0.35	0.21
Ca	0.18	0.29	0.36	0.30	0.42	0.41	0.51	0.32	0.18
Cl	0.12	0.28	0.33	0.28	0.38	0.36	0.47	0.26	0.10
EC	0.18	0.29	0.36	0.30	0.41	0.41	0.51	0.32	0.18
Fe	0.20	0.32	0.39	0.33	0.45	0.44	0.54	0.35	0.21
K	0.18	0.29	0.36	0.30	0.42	0.41	0.51	0.32	0.18
Mg	0.18	0.29	0.36	0.30	0.42	0.41	0.51	0.32	0.18
Mn	0.20	0.32	0.39	0.33	0.45	0.44	0.54	0.35	0.21
Na	0.18	0.29	0.36	0.30	0.42	0.41	0.51	0.32	0.18
OC	0.18	0.30	0.36	0.30	0.42	0.41	0.51	0.32	0.18
Si	0.20	0.32	0.39	0.33	0.45	0.44	0.54	0.35	0.21
Ti	0.20	0.32	0.39	0.33	0.45	0.44	0.54	0.35	0.21
NH_4^+	-12.28	-16.94	-19.80	-16.35	-20.68	-20.35	-23.34	-17.89	-8.93
NO_3^-	1.23	1.63	1.54	1.36	1.35	1.50	1.14	1.66	1.96
SO_4^{2-}	0.21	0.32	0.40	0.33	0.48	0.48	0.62	0.39	0.19
Other	0.18	0.29	0.36	0.30	0.42	0.41	0.51	0.33	0.18

δ_i represent the sensitivity coefficients (δ) of simulated components in case DBL at monitoring site i.

TE13

Fig. 8: The cyan colours are difficult to distinguish.

We have modified the cyan color scheme to distinguish between them (Fig. TE12 below).

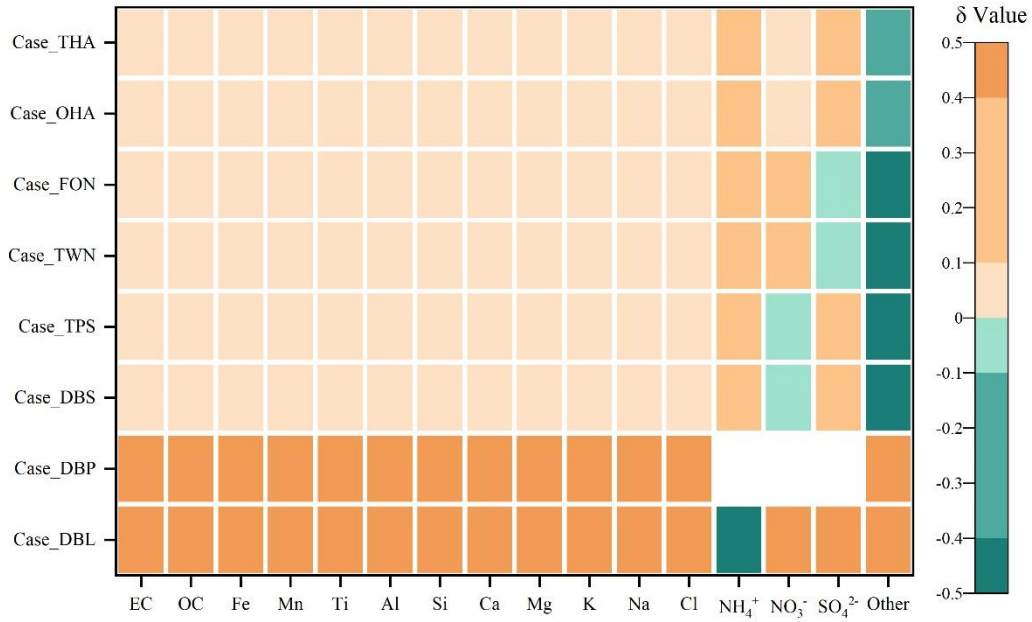


Fig. TE12 The sensitivity coefficients (δ) of simulated components to the perturbation of adopted source profile in different cases. Note: Each small color box in the figure represented the sensitivity level (indicated by the legend on the right) of PM_{2.5} components (the x-coordinate) in different cases (y-coordinate). The blank grids in DBP case indicated no perturbation to SNA in PM_{2.5} source profile under this case.

TE14

Line 450: Please insert the Eqs. (3) to (5) after "parameters" and adjust the following sentences accordingly.

Thank you for your advice. We have inserted the meaning of each parameter as follow:

$$R_1 = \frac{[NH_4^+] + [Ca^{2+}] + [K^+] + [Mg^{2+}] + [Na^+]}{[SO_4^{2-}]} \dots\dots\dots (1)$$

$$R_2 = \frac{[Ca^{2+}] + [K^+] + [Mg^{2+}] + [Na^+]}{[SO_4^{2-}]} \dots\dots\dots (2)$$

$$R_3 = \frac{[Ca^{2+}] + [K^+] + [Mg^{2+}]}{[SO_4^{2-}]} \dots\dots\dots (3)$$

Where [X] denotes the molar concentration of component (mol m⁻³), R₁, R₂ and

R₃ are termed “total sulfate ratio”, “crustal species and sodium ratio” and “crustal species ratio” respectively; Based on their values, some aerosol composition regimes are defined (Detailed rules are defined in Table TE17. It has also been added in Table S27 of our supplementary material).

Table TE17 Five aerosol types in ISORROPIA and corresponding R value

R ₁	R ₂	R ₃	Aerosol type	Solid phase
R ₁ <1	any value	any value	Sulfate Rich (free acid)	NaHSO ₄ , NH ₄ HSO ₄ , KHSO ₄ , CaSO ₄
1≤R ₁ ≤2	any value	any value	Sulfate Rich	NaHSO ₄ , NH ₄ HSO ₄ , Na ₂ SO ₄ , (NH ₄) ₂ SO ₄ , (NH ₄) ₃ H(SO ₄) ₂ , CaSO ₄ , KHSO ₄ , K ₂ SO ₄ , MgSO ₄
R ₁ ≥2	R ₂ <2	any value	Sulfate Poor, Crustal & Sodium Poor	Na ₂ SO ₄ , (NH ₄) ₂ SO ₄ , NH ₄ NO ₃ , NH ₄ Cl, CaSO ₄ , K ₂ SO ₄ , MgSO ₄
R ₁ ≥2	R ₂ ≥2	R ₃ <2	Sulfate Poor, Crustal & Sodium Rich, Crustal Poor	Na ₂ SO ₄ , NaNO ₄ , NaCl, NH ₄ NO ₃ , NH ₄ Cl, CaSO ₄ , K ₂ SO ₄ , MgSO ₄
R ₁ ≥2	R ₂ ≥2	R ₃ >2	Sulfate Poor, Crustal & Sodium Rich, Crustal Rich	NaNO ₄ , NaCl, NH ₄ NO ₃ , NH ₄ Cl, CaSO ₄ , K ₂ SO ₄ , MgSO ₄ , Ca(NO ₃) ₂ , CaCl ₂ , Mg(NO ₃) ₂ , MgCl ₂ , KNO ₃ , KCl

Source: Fountoukis and Nenes, 2007

TE15

Table 2: Please specify if these are averages. Given the variability of the simulations, it is not clear how representative these values are.

Thank you for your advice.

R₁, R₂ and R₃ represent the “total sulfate ratio”, “crustal species and sodium ratio” and “crustal species ratio” respectively. R₁’s value is determined by molar concentration of NH₄⁺, Ca²⁺, K⁺, Mg²⁺, Na⁺ and SO₄²⁻, R₂ is controlled by Ca²⁺, K⁺, Mg²⁺, Na⁺ and SO₄²⁻, R₃ is influenced by Ca²⁺, K⁺, Mg²⁺ and SO₄²⁻ (Equation 1~3 below).

$$R_1 = \frac{[\text{NH}_4^+] + [\text{Ca}^{2+}] + [\text{K}^+] + [\text{Mg}^{2+}] + [\text{Na}^+]}{[\text{SO}_4^{2-}]} \dots\dots\dots (1)$$

$$R_2 = \frac{[Ca^{2+}] + [K^+] + [Mg^{2+}] + [Na^+]}{[SO_4^{2-}]} \dots\dots\dots (2)$$

$$R_3 = \frac{[Ca^{2+}] + [K^+] + [Mg^{2+}]}{[SO_4^{2-}]} \dots\dots\dots (3)$$

Where [X] denotes molar concentration of component (mol·m⁻³)

The values of R₁, R₂ and R₃ in Table 2 are monthly average values during Oct.1~Oct. 30 in 2018. Based on their values, the aerosol composition regimes in the model are defined. The model introduced the values of R to define the simulation subsystems and potential aerosol species, then discuss the influence pathway of source profile perturbation on simulated PM_{2.5} components and linkage mechanism among components.

We also add Table TE18 below to illustrate the content of sensitivity experiment, potential aerosol species in ISORROPIA II under different cases, then to make this question clearly.

Table TE18 The content of sensitivity experiment, potential aerosol species in ISORROPIA II under different cases

Experiment Cases	Description ³	R ₁	R ₂	R ₃	Solid phase species
Case SGL	Base case	2.53	2.52	1.9	CaSO ₄ , MgSO ₄ , K ₂ SO ₄ , Na ₂ SO ₄ , NaCl, NaNO ₃ , NH ₄ Cl, NH ₄ NO ₃
Case DBL: add perturbation to Non-SNA and SNA ¹	The percentage of all the listed components in the source profile of base case (SGL) were doubled, and the proportion of unlisted components (Other) ² decreased to 9%.	2.53	2.52	1.9	CaSO ₄ , MgSO ₄ , K ₂ SO ₄ , Na ₂ SO ₄ , NaCl, NaNO ₃ , NH ₄ Cl, NH ₄ NO ₃
Case DBP: add perturbation to Non-SNA	The percentages of non-SNA were doubled and SNA(SO ₄ ²⁻ , NO ₃ ⁻ , NH ₄ ⁺) species stayed the same with that in SGL (the cumulative percentage of listed species was 85.3%), the proportion of unlisted components decreased to 14.7%.	5.04	5.03	3.79	CaSO ₄ , MgSO ₄ , K ₂ SO ₄ , CaCl ₂ , Ca(NO ₃) ₂ , MgCl ₂ , Mg(NO ₃) ₂ , KCl, KNO ₃ , NaCl, NaNO ₃ , NH ₄ Cl, NH ₄ NO ₃
Case DBS: add perturbation to SO ₄ ²⁻	The percentage of SO ₄ ²⁻ was doubled (11%, DBS, represented Double Sulfate) and the other listed 14 species stayed the same with that in SGL (the cumulative percentage of listed species was 51%), the proportion of unlisted components decreased to 49%.	1.26	1.26	0.95	CaSO ₄ , MgSO ₄ , K ₂ SO ₄ , KHSO ₄ , Na ₂ SO ₄ , NaHSO ₄ , (NH ₄) ₂ SO ₄ , NH ₄ HSO ₄ , (NH ₄) ₃ H(SO ₄) ₂
Case TPS: add perturbation to SO ₄ ²⁻	The percentage of SO ₄ ²⁻ was tripled (16.5%, TPS, represented Triple Sulfate) and the other listed 14 species stayed the same with that in SGL (the cumulative percentage of listed species was 57%), the proportion of unlisted components decreased to 43%.	0.84	0.84	0.63	CaSO ₄ , KHSO ₄ , NaHSO ₄ , NH ₄ HSO ₄

Case TWN: add perturbation to NO ₃ ⁻	The NO ₃ ⁻ content was raised up to 20 times (3.3%, TWN) of that in SGL (0.16%), the other 14 species stayed the same with SGL (the cumulative percentage of listed species was 48.6%), the proportion of unlisted components decreased to 51.4%.	2.53	2.52	1.9	CaSO ₄ , MgSO ₄ , K ₂ SO ₄ , Na ₂ SO ₄ , NaCl, NaNO ₃ , NH ₄ Cl, NH ₄ NO ₃
Case FON: add perturbation to NO ₃ ⁻	The NO ₃ ⁻ content was raised up to 40 times (6.6%, FON) of that in SGL (0.16%), the other 14 species stayed the same with SGL (the cumulative percentage of listed species was 51.9%), the proportion of unlisted components decreased to 48.1%.	2.53	2.52	1.9	CaSO ₄ , MgSO ₄ , K ₂ SO ₄ , Na ₂ SO ₄ , NaCl, NaNO ₃ , NH ₄ Cl, NH ₄ NO ₃
Case OHA: add perturbation to NH ₄ ⁺	The NH ₄ ⁺ content was raised up to 100 times (2.2%, OHA) of that in SGL (0.02%), the other 14 species stayed the same with SGL (the cumulative percentage of listed species was 47.7%), the proportion of unlisted components decreased to 52.3%.	3.58	2.52	2.95	CaSO ₄ , MgSO ₄ , K ₂ SO ₄ , CaCl ₂ , Ca(NO ₃) ₂ , MgCl ₂ , Mg(NO ₃) ₂ , KCl, KNO ₃ , NaCl, NaNO ₃ , NH ₄ Cl, NH ₄ NO ₃
Case THA: add perturbation to NH ₄ ⁺	The NH ₄ ⁺ content was raised up to 200 times (4.4%, THA) of that in SGL (0.02%), the other 14 species stayed the same with SGL (the cumulative percentage of listed species was 49.9%), the proportion of unlisted components decreased to 50.1%.	4.64	2.52	4.02	CaSO ₄ , MgSO ₄ , K ₂ SO ₄ , CaCl ₂ , Ca(NO ₃) ₂ , MgCl ₂ , Mg(NO ₃) ₂ , KCl, KNO ₃ , NaCl, NaNO ₃ , NH ₄ Cl, NH ₄ NO ₃

Note:

1. SNA represent SO₄²⁻, NO₃⁻, and NH₄⁺, Non-SNA represent other components in PM_{2.5}.
2. The listed components contain Al, Ca, Cl, EC, Fe, K, Mg, Mn, Na, OC, Si, Ti, NH₄⁺, NO₃⁻ and SO₄²⁻, unlisted components are classified as Other.
3. The source profiles in all cases listed in the table were calculated based on the base case SGL. In the design of simulation cases, the reason why the disturbance amplitude of NH₄⁺ and NO₃⁻ were significantly higher than that of other components such as SO₄²⁻ and Non-SNA, was because the percentages of NH₄⁺ and NO₃⁻

in the base source profile (SGL, based on the chemical composition of code 000002.5 in the EPA Speciate_5.0_0 database) were very low, while the percentage of NH_4^+ and NO_3^- in SPAPPC exhibited in section 2.2 were orders of magnitude higher than those in SGL.

TE16

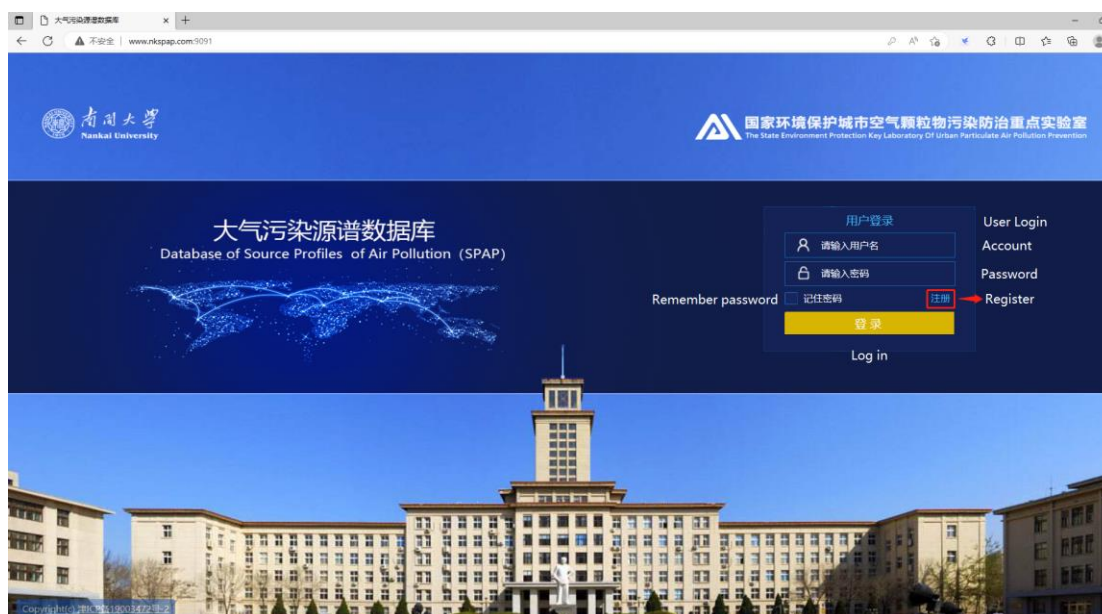
Data availability section: Please provide all inputs and model configuration data necessary to reproduce the results as well as all output data discussed in the article in a suitable data repository (e.g., Zenodo, see also https://www.geoscientific-model-development.net/policies/code_and_data_policy.html). For many readers, the SPAP database is behind a language barrier, please consider other ways to make it accessible (e.g., if the license allows, provide the relevant data in another repository).

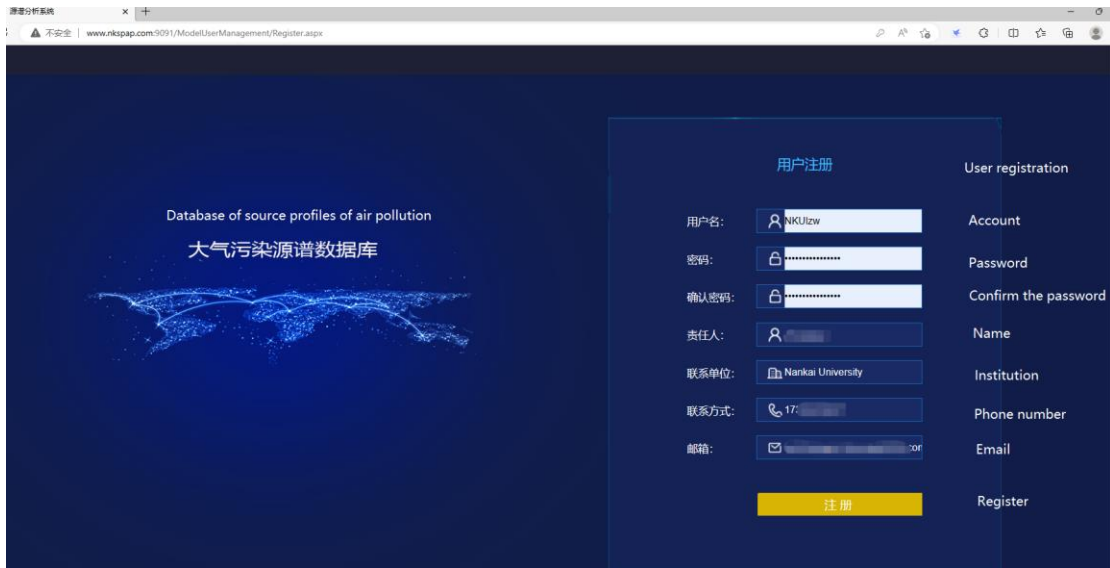
Thank you for your advice. We have provided all inputs and model configuration data necessary in Zenodo (<https://zenodo.org/record/7865675>). We also provide the tutorial guide (English version) for better use SPAP database. Furthermore, the English version of SPAP database has already proceed but still need some time. It will be accessible in the near future for more widely readers.

The tutorial guide is shown as follows:

Step1: Register

Access the site by typing the address “<http://www.nkspap.com:9091/>” through Google Chrome, Microsoft Edge, or other available web browser. (Or use our test account: [Account: NKUtest; Password: NKUtest2023])





Step 2: Log in





Step 3: View, download recommend source profile

Click the Data analysis window. Then click the [Data query] or [Recommend source profile] module.



Besides that, this page also contains statistical analysis and similarity analysis function which can draw column, column deviation or stacked area charts.

Reference

- Appel, K. W., Poulio, G. A., Simon, H., Sarwar, G., Pye, H. O. T., Napelenok, S. L., Akhtar, F., Roselle, S. J.: Evaluation of dust and trace metal estimates from the Community Multiscale Air Quality (CMAQ) model version 5.0, *Geosci. Model Dev.*, 6, 883-899, <https://doi.org/10.5194/gmd-6-883-2013>, 2013.
- Bao, Z., Feng, Y. C., Jiao, Q., Hong, S. M., Liu, W. G.: Characterization and Source Apportionment of PM_{2.5} and PM₁₀ in Hangzhou (In Chinese), *Environ. Monitor. China*, 26, 47-51, <https://doi.org/10.19316/j.issn.1002-6002.2010.02.012>, 2010.
- Bi, X., Dai, Q., Wu, J., Zhang, Q., Zhang, W., Luo, R., Cheng, Y., Zhang, J., Wang, L., Yu, Z., Zhang, Y., Tian, Y., Feng, Y.: Characteristics of the main primary source profiles of particulate matter across China from 1987 to 2017, *Atmos. Chem. Phys.*, 19, 3223-3243, <https://doi.org/10.5194/acp-19-3223-2019>, 2019.
- Bray, C., Strum, M., Simon, H., Riddick, L., Kosusko, M., Menetrez, M., Hays, M., Rao, V.: An assessment of important SPECIATE profiles in the EPA emissions modeling platform and current data gaps, *Atmos. Environ.*, 207, 93-104, <https://doi.org/10.1016/j.atmosenv.2019.03.013>, 2019.
- Chapel Hill, N.: Operational Guidance for the Community Multiscale Air Quality (CMAQ) Modeling System Version 5.0, [https://www.airqualitymodeling.org/index.php/CMAQ_version_5.0_\(February_2010_release\)_OGD#Aerosol_Module](https://www.airqualitymodeling.org/index.php/CMAQ_version_5.0_(February_2010_release)_OGD#Aerosol_Module), last access: February 2012.
- Chen, J., Yin, D., Zhao, Z., Kaduwela, A. P., Avise, J. C., Damassa, J. A., Beyersdorf, A., Burton, S., Ferrare, R., Herman, J. R., Kim, H., Neuman, A., Nowak, J. B., Parworth, C., Scarino, A. J., Wisthaler, A., Young, D. E., Zhang, Q.: Modeling air quality in the San Joaquin valley of California during the 2013 Discover-AQ field campaign, *Atmos. Environ.*, 5, 100067, <https://doi.org/10.1016/j.aeaoa.2020.100067>, 2020.
- Cheng, N. L., Meng, F., Wang, J. K., Chen, Y. B., Wei, X., Han, H.: Numerical simulation of the spatial distribution and deposition of PM_{2.5} in East China coastal area in 2010 (In Chinese), *Journ. Safety Environ.*, 15, 305-310, <https://doi.org/10.13637/j.issn.1009-6094.2015.06.063>, 2015.
- Cui, H.: Study of chemical composition features and sources apportionment of airborne particles during heating period in Jincheng city (In Chinese). Taiyuan University of Technology, Taiyuan.2011
- Cui, M., Chen, Y., Feng, Y., Li, C., Zheng, J., Tian, C., Yan, C., Zheng, M.: Measurement of PM and its chemical composition in real-world emissions from non-road and on-road diesel vehicles, *Atmospheric Chemistry and Physics*, 17, 6779-6795, <https://doi.org/10.5194/acp-17-6779-2017>, 2017.
- Dai, Q., Bi, X., Song, W., Li, T., Liu, B., Ding, J., Xu, J., Song, C., Yang, N., Schulze, B. C., Zhang, Y., Feng, Y., Hopke, P. K.: Residential coal combustion as a source of primary sulfate in Xi'an, China, *Atmos. Environ.*, 196, 66-76, <https://doi.org/10.1016/j.atmosenv.2018.10.002>, 2019.
- Feng, X. Q.: Source characteristics of VOCs and PM_{2.5} for vehicle exhausts in the Pearl River Delta region (In Chinese). South China University of Technology, Guangzhou.2013
- Foley, K. M., Roselle, S. J., Appel, K. W., Bhave, P. V., Pleim, J., Otte, T., Mathur, R., Sarwar, G., Young, J. O., Gilliam, R.: Incremental testing of the community multiscale air quality (CMAQ) modeling system version 4.7, *Geosci. Model Dev.*, 3, 205-226, <https://doi.org/10.5194/gmd-3-205-2010>, 2010.
- Fountoukis, C., Nenes, A.: ISORROPIA II: a computationally efficient thermodynamic equilibrium

- model for K^+ - Ca^{2+} - Mg^{2+} - NH_4^+ - Na^+ - SO_4^{2-} - NO_3^- - Cl^- - H_2O aerosols, *Atmos. Chem. Phys.*, 7, 4639-4659, <https://doi.org/10.5194/acp-7-4639-2007>, 2007.
- Friberg, M. D., Zhai, X., Holmes, H. A., Chang, H. H., Strickland, M. J., Sarnat, S. E., Tolbert, P. E., Russell, A. G., Mulholland, J. A.: Method for Fusing Observational Data and Chemical Transport Model Simulations To Estimate Spatiotemporally Resolved Ambient Air Pollution, *Environ. Sci. Technol.*, 50, 3695-3705, <https://doi.org/10.1021/acs.est.5b05134>, 2016.
- Gao, Y., Shan, H., Zhang, S., Sheng, L., Li, J., Zhang, J., Ma, M., Meng, H., Luo, K., Gao, H., Yao, X.: Characteristics and sources of $PM_{2.5}$ with focus on two severe pollution events in a coastal city of Qingdao, China, *Chemosphere*, 247, 125861, <https://doi.org/10.1016/j.chemosphere.2020.125861>, 2020.
- Ge, S., Xu, X., Chow, J. C., Watson, J., Sheng, Q., Liu, W., Bai, Z., Zhu, T., Zhang, J.: Emissions of air pollutants from household stoves: honeycomb coal versus coal cake, *Environ. Sci. Technol.*, 38, 4612-4618, <https://doi.org/10.1021/es049942k>, 2004.
- Gong, P., Luo, Y.: Study on the characteristics of source profiles in Wuhan (In Chinese), *J. Nanjing University of Information Sci. Technol.*, 10, 579-589, <https://doi.org/10.13878/j.cnki.jnuist.2018.05.008>, 2018.
- Guo, Y., Zheng, Y., Zhu, T., Gao, X., Luo, L., Zheng, Y.: Chemical profiles of PM emitted from the iron and steel industry in northern China, *Atmos. Environ.*, 150, 187-197, <https://doi.org/10.1016/j.atmosenv.2016.11.055>, 2017.
- Hao, Y., Gao, C., Deng, S., Yuan, M., Song, W., Lu, Z., Qiu, Z.: Chemical characterisation of $PM_{2.5}$ emitted from motor vehicles powered by diesel, gasoline, natural gas and methanol fuel, *Sci. Total Environ.*, 674, 128-139, <https://doi.org/10.1016/j.scitotenv.2019.03.410>, 2019.
- Ho, K. F., Lee, S. C., Chow, J. C., Watson, J. G.: Characterization of PM_{10} and $PM_{2.5}$ source profiles for fugitive dust in Hong Kong, *Atmos. Environ.*, 37, 1023-1032, [https://doi.org/10.1016/s1352-2310\(02\)01028-2](https://doi.org/10.1016/s1352-2310(02)01028-2), 2003.
- Kong, S. F.: Study on the chemical composition, risk assessment and emission inventory establishment for hazardous components in particulate matter from atmospheric pollution sources (In Chinese). Nankai University, Tianjin 2012
- Li, J., Han, Z., Li, J., Liu, R., Wu, Y., Liang, L., Zhang, R.: The formation and evolution of secondary organic aerosol during haze events in Beijing in wintertime, *Sci. Total Environ.*, 703, 134937, <https://doi.org/10.1016/j.scitotenv.2019.134937>, 2020.
- Liu, X. H., Zhang, Y., Olsen, K. M., Wang, W. X., Do, B. A., Bridgers, G. M.: Responses of future air quality to emission controls over North Carolina, Part I: Model evaluation for current-year simulations, *Atmos. Environ.*, 44, 2443-2456, <https://doi.org/10.1016/j.atmosenv.2010.04.002>, 2010.
- Liu, X. Y.: Emission characteristics of particulate matter from typical fixed combustion sources. Chinese Academy of Environmental Sciences, Beijing.2007
- Liu, Y., Zhang, W., Yang, W., Bai, Z., Zhao, X.: Chemical Compositions of $PM_{2.5}$ Emitted from Diesel Trucks and Construction Equipment, *Aerosol Sci. Eng.*, 2, 51-60, <https://doi.org/10.1007/s41810-017-0020-2>, 2018.
- Liu, Y. Y., Zhang, W. J., Bai, Z. P., Yang, W., Zhao, X., Han, B., Wang, X.: Characteristics of $PM_{2.5}$ Chemical Source Profiles of Coal Combustion and Industrial Process in China (In Chinese), *Res. Environ. Sci.*, 30, 1859-1868, <https://doi.org/10.13198/j.issn.1001-6929.2017.03.34>, 2017.
- Ma, J. H.: Emission characteristics of particulates from typical production process of iron and steel

- enterprises. Xinan University, Chongqing.2009
- Ma, Z., Liang, Y., Zhang, J., Zhang, D., Liu, B.: PM_{2.5} profiles of typical sources in Beijing (In Chinese), *Acta Scientiae Circumstantiae*, 35, 4043-4052, <https://doi.org/10.13671/j.hjkxxb.2015.0584>, 2015.
- Nenes, A., Pandis, S. N., Pilinis, C.: ISORROPIA: A New Thermodynamic Equilibrium Model for Multiphase Multicomponent Inorganic Aerosols, *Aquat. Geochem.*, 4, 123-152, <https://doi.org/10.1023/A:1009604003981>, 1998.
- Qi, K., Dai, C., Feng, Y., Yang, L.: Establishment and analysis of PM_{2.5} industrial source profiles in Shijiazhuang City (In Chinese), *Hebei J. Ind. Sci. Technol.*, 32, 78-84, <https://doi.org/10.7535/hbgykj.2015yx01014>, 2015.
- Reff, A., Bhave, P. V., Simon, H., Pace, T. G., Pouliot, G. A., Mobley, J. D., Houyoux, M.: Emissions Inventory of PM_{2.5} Trace Elements across the United States, *Environ. Sci. Technol.*, 43, 5790-5796, <http://doi.org/10.1021/es802930x>, 2009.
- Sha, T., Ma, X., Jia, H., Tian, R., Chang, Y., Cao, F., Zhang, Y.: Aerosol chemical component: Simulations with WRF-Chem and comparison with observations in Nanjing, *Atmos. Environ.*, 218, 1-14, <https://doi.org/10.1016/j.atmosenv.2019.116982>, 2019.
- Shi, Z., Li, J., Huang, L., Wang, P., Wu, L., Ying, Q., Zhang, H., Lu, L., Liu, X., Liao, H., Hu, J.: Source apportionment of fine particulate matter in China in 2013 using a source-oriented chemical transport model, *Sci. Total Environ.*, 601-602, 1476-1487, <https://doi.org/10.1016/j.scitotenv.2017.06.019>, 2017.
- Teng, J. Q., Wang, W., Jiang, S. J., Cheng, Z., Xue, Y. G.: Study on the Source Profiles of PM_{2.5} Major Emissions in Changzhou (In Chinese), *Environ. Sci. Technol.*, 28, 56-59+64, 2015.
- Wang, G., Lang, J., Cheng, S., Yao, S., Wang, X.: Characteristics of PM_{2.5} and hydrocarbon emitted from heavy-duty diesel vehicle (In Chinese), *China Environ. Sci.*, 35, 3581-3587, <https://doi.org/10.3969/j.issn.1000-6923.2015.12.007>, 2015.
- Wang, Z., Guo, J., Chen, Z.: Analysis of the source componential spectrum of PM_{2.5} emission in Guiyang (In Chinese), *J. Safety Environ.*, 16, 346-351, <https://doi.org/10.13637/j.issn.1009-6094.2016.02.069>, 2016.
- Wen, J., Li, B., Zhang, X., Tian, Y., Huang, B., Zhu, H., Feng, Y.: PM_{2.5} Profiles of Typical Industrial Emissions in Yantai City, China (In Chinese), *Res. Environ. Sci.*, 32, 1333-1339, <https://doi.org/10.13198/j.issn.1001-6929.2019.04.06>, 2019.
- Wen, J., Yang, J., Li, P., Yu, J., Wu, J., Feng, Y.: Chemical Source Profiles of PM Emitted from the Main Processes of the Iron and Steel Industry in China (In Chinese), *Environ. Sci.*, 39, 4885-4891, <https://doi.org/10.13227/j.hjkx.201804007>, 2018.
- Xing, J., Mathur, R., Pleim, J., Hogrefe, C., Gan, C. M., Wong, D. C., Wei, C., Gilliam, R., Pouliot, G.: Observations and modeling of air quality trends over 1990–2010 across the Northern Hemisphere: China, the United States and Europe, *Atmos. Chem. Phys.*, 15, 2723-2747, <https://doi.org/10.5194/acp-15-2723-2015>, 2015.
- Ye, M., Guo, Y., Zhu, T., Luo, L., Du, Q.: Research on the characteristics of particulate matter emitted from the cement plants (In Chinese), *Environ. Engineering*, 35, 346-352, 2017.
- Zhang, N., Zhuang, M., Tian, J., Tian, P., Zhang, J., Wang, Q., Zhou, Y., Huang, R., Zhu, C., Zhang, X., Cao, J.: Development of source profiles and their application in source apportionment of PM_{2.5} in Xiamen, China, *Front. Environ. Sci. Eng.*, 10, 1-13, <https://doi.org/10.1007/s11783-016-0879-1>, 2016.
- Zhang, P. F.: Study on composition source profile and characteristics of particulate matter from diesel

- Bus exhaust in Tianjin (In Chinese). Nankai University, Tianjin 2007
- Zhang, Q., Xue, D., Wang, S., Wang, L., Wang, J., Ma, Y., Liu, X.: Analysis on the evolution of PM_{2.5} heavy air pollution process in Qingdao (In Chinese), *China Environ. Sci.*, 37, 3623-3635, <https://doi.org/10.3969/j.issn.1000-6923.2017.10.003>, 2017.
- Zhang, Y., Olsen, K. M., Wang, K.: Fine Scale Modeling of Agricultural Air Quality over the Southeastern United States Using Two Air Quality Models. Part I. Application and Evaluation, *Aerosol Air Qual. Res.*, 13, 1231-1252, <https://doi.org/10.4209/aaqr.2012.12.0346>, 2013.
- Zhang, Y., Yao, Z., Shen, X., Liu, H., He, K.: Chemical characterization of PM_{2.5} emitted from on-road heavy-duty diesel trucks in China, *Atmospheric Environment*, 122, 885-891, <https://doi.org/10.1016/j.atmosenv.2015.07.014>, 2015.
- Zhao, H. N.: The emission characteristic and reduction strategies study on PM_{2.5} of ferrous metal smelting (steel) industry. North China Electric Power University, Baoding.2014
- Zheng, B., Zhang, Q., Zhang, Y., He, K. B., Wang, K., Zheng, G. J., Duan, F. K., Ma, Y. L., Kimoto, T.: Heterogeneous chemistry: a mechanism missing in current models to explain secondary inorganic aerosol formation during the January 2013 haze episode in North China, *Atmos. Chem. Phys.*, 15, 2031-2049, <https://doi.org/10.5194/acp-15-2031-2015>, 2015.
- Zheng, M., Zhang, Y., Yan, C., Fu, H., Niu, Y., Huang, K., Hu, M., Zeng, L., Liu, Q., Pei, B., Fu, Q.: Establishing PM_{2.5} industrial source profiles in Shanghai (In Chinese), *China Environ. Sci.*, 33, 1354-1359, <https://doi.org/10.3969/j.issn.1000-6923.2013.08.002>, 2013.